主論文

(Regular Paper)

Physiological and Clinical Chemistry, and Nutrition

Changes in Aerobic and Anaerobic ATP-Synthesizing Activities in Hypoxic Mouse Brain[1]

Hirokazu Ueda,* Tadao Hashimoto,* Eisuke Furuya,*
Kunio Tagawa,*[2] Kazuo Kitagawa,** Masayasu Matsumoto,**
Shotaro Yoneda,** Kazufumi Kimura,** and Takenobu Kamada**

*Department of Physiological Chemistry, and **First Department of Internal Medicine, Medical School, Osaka University, Kita-ku, Osaka, Osaka 530

原稿 23枚，表 3枚．図 5枚．

連絡先：530 大阪市北区中之島 4-3-57
大阪大学分子生理化学教室
田川邦夫
電話 06(443)5531 内線 382

Running Title: Energy metabolism in hypoxic brain

[1]This work was supported in part by Grants-in-Aid for Scientific Research (no. 61480130 and no. 62222013) from the Ministry of Education, Science, and Culture of Japan.

[2]To whom correspondence should be addressed.

Abbreviations: $\Delta\sim P$, cerebral rate of utilization of high energy phosphate bonds; P-Cr, creatine phosphate; FiO_2, inspired oxygen concentration; PaO_2, arterial oxygen pressure

SUMMARY

The changes in cerebral metabolism in mice in severe hypoxia were investigated by analyses of changes in the levels of energy metabolites and near infrared spectrophotometric assessment of the states of hemoglobin and cytochrome oxidase. Under 4.4% O_2, the contribution of anaerobic ATP production was at most about 20% of the demand. However, the cerebral ATP level was kept at the control level until about one minute before death. Pentobarbital anaesthesia, which reduced the cerebral rate of metabolism, prolonged the survival time, although anaerobic ATP production still did not support ATP demand. In these conditions, deoxygenation of hemoglobin and reduction of cytochrome oxidase proceeded rapidly within one minute. Hemoglobin reached the maximum state of deoxygenation in the middle phase of hypoxia, with no further change until death. However, cytochrome oxidase was reduced slowly with one phase of partial reoxidation due to increase of cerebral blood volume, and reached the completely reduced state at death. From these results it was concluded that the aerobic ATP synthesis, which supplied more than 80% of the cerebral demand, was inferred to decrease gradually because of limitation of oxygen supply, and that the failure of oxidative phosphorylation to meet demand triggered decrease in the cellular ATP level that led to death.

There have been many studies on the effects of hypoxia on energy metabolism in the brain. Results have shown that the cerebral ATP level remains almost constant until the inspired oxygen content (FiO_2) decreases to 4% (1), or the arterial oxygen pressure (PaO_2) to 15-20 mmHg (2,3), although the creatine phosphate (P-Cr) level decreases and lactate accumulates at an FiO_2 of 7% (1) and PaO_2 of 35-40 mmHg (2,3). These results indicate that energy balance is well maintained even in severe hypoxia. Consistent with this, many laboratories have reported the existence of compensation mechanisms, such as decrease in energy demand (4,5), acceleration of glycolysis (6,7), and increase of cerebral blood flow for increasing the supply of oxygen (8-10). As Johannsson and Siesjo pointed out, increase in the efficiency of the oxygen supply system seems the most significant compensatory mechanism for meeting the cerebral energy demand under hypoxia (9), although lactic accumulation or activation of anaerobic glycolysis are marked features as reflections of decrease in oxygen consumption (6). However, under severe hypoxia, the energy balance cannot be maintained for long and the cerebral ATP level decreases, leading to death (11). There are no reports on how this energy failure occurs and proceeds, leading to death.

Recently, near-infrared spectrophotometry has been shown to be very useful for analyzing the state of oxygenation of hemoglobin and the redox state of cytochrome oxidase in vivo (12-17). In the present study, we used this method to follow changes in oxygen metabolism in hypoxic mouse brain, where in spite of increased blood flow during hypoxia, cytochrome oxidase was gradually reduced and reached the level of complete reduction at

death. We also analyzed changes in the cerebral levels of high energy compounds under various conditions. The results showed that anaerobic glycolysis, even when increased several-fold, contributed only in small part to the total cerebral energy demand, which must mainly be supplied by aerobic metabolism even under severe hypoxia. The decrease in the cerebral ATP level in the late stage of severe hypoxia, which led directly to death, was found to be caused by decrease in oxidative phosphorylation activity due to the reduced oxygen supply.

MATERIALS AND METHODS

Animals and sampling procedures--Adult male ddY mice, weighing about 20g, were maintained with free access to standard laboratory chow and tap water. Hypoxic conditions were introduced without any anaesthetic, by placing the mice in a chamber (about 500 ml) connected to a mixed gas cylinder that supplied a mixture of oxygen and nitrogen at a constant flow rate of 1.5 l/min. For induction of anaesthesia, sodium pentobarbital (Nembutal, Abbott Laboratories, U.S.A.) at a dose of 30 mg/kg body weight was injected intraperitoneally (i.p.) 10 minutes before the experiment. Hyperglycemia was induced by i.p. injection of 0.6 ml of 2.8 M glucose solution one hour before exposure to hypoxia. The survival time was defined as the time until respiratory failure. The clinical course of hypoxic death was as described by others (4). At the indicated times, the brain was frozen by immersing the mice head-first in liquid nitrogen to minimize metabolic changes (18). Then the brain was chiselled

out, lyophilized overnight, and kept in a desiccator at -80°C until analyzed. The lyophilized brain was weighed (dry weight) and homogenized in 0.5 M perchloric acid. The homogenate was centrifuged at 10,000g for 10 min, and the supernatant was neutralized with 1 M potassium hydroxide. The resultant precipitate was removed by centrifugation and the supernatant was used as the test sample. The extraction procedures described above were done at 0°C.

Assay methods--ATP and ADP levels were determined by HPLC, as reported previously (19). AMP was determined using a reverse phase HPLC column (Microsorb C_{18}, 0.4 cm x 15 cm, Rainin Instrument Co., U.S.A.), which was equilibrated with 0.4 M NaH_2PO_4 at a flow rate of 1.0 ml/min. AMP was detected at 9.6 min by change in the absorbance at 260 nm. Creatine phosphate was assayed using an anion exchanger DEAE-2SW column (0.4 cm x 25 cm, Tosoh Co., Japan), which was equilibrated with 80 mM sodium phosphate buffer, pH 6.0. The column was developed at a flow rate of 1.0 ml/min, and creatine phosphate, monitored by its absorbance at 210 nm, was eluted at 10.0 min. The sensitivities of the assays of AMP and creatine phosphate were similar to those of the assays of ATP and ADP. Lactate was determined by a newly developed electrochemical method. The apparatus consisted of a column of immobilized lactate oxidase (L-lactate: oxygen oxidoreductase, EC 1.1.3.2) from Pediococcus sp. and an H_2O_2 electrode. The principle of this method was the same as that of the method for measuring glucose described previously (20), but with lactate oxidase instead of glucose oxidase (β-D-glucose: oxygen 1-oxidoreductase, EC 1.1.3.4). However, brain samples contain

large amounts of reducing substances, such as ascorbic acid, that react with the electrode. Therefore, these substances were first removed on a DEAE-2SW column equilibrated with 80 mM sodium phosphate buffer, pH 6.0. The retention time of lactate was 7.8 min at a flow rate of 0.75 ml/min. With this system, 0.05-1.0 nmol of L-lactate could be determined precisely. D-Lactate and other organic acids did not react with the enzyme. In glucose determination, the retention time was 5.0 min. A sample of 3 mg of dry tissue was sufficient for analyses of all these substances. The cyclic AMP level was determined by HPLC with a C_{18} column equilibrated with 0.4 M NaH_2PO_4 containing 4% acetonitrile, and the absorption of the eluate at 260 nm was measured. At a flow rate of 0.5 ml, cyclic AMP was eluated at 17.0 min and 1 pmol of this substance could be determined. The fructose 2,6-bisphosphate level was determined enzymatically (21).

Calculation of metabolic rates--As described by Lowry et al. (22), the cerebral energy demand, or the rate of utilization of high energy phosphate bonds (Δ~P), could be calculated from the initial velocity of change in the high energy phosphate level during complete ischemia (decapitation), according to the formula; $\Delta \sim P = \Delta PCr + 2 \times \Delta ATP + \Delta ADP - \Delta$ Lactate. Thus, we plotted the levels of total high energy phosphate compounds minus lactate ($\Sigma(\sim P) = PCr + 2 \times ATP + ADP -$ Lactate) against the time after decapitation, and from the slope, determined the rate of energy utilization. As reported previously (5,23), the metabolite levels on in situ freezing (see above) were different from those of brain frozen soon after decapitation. This difference was due to the time required for freezing the brain tissue (5-10

sec). The best linear relationship was obtained for our data assuming a freezing time of 7.5 sec. Thus, data in Fig. 2 were plotted against the "real" ischemic time, taken as the time after decapitation plus 7.5 sec. The aerobic glycolytic rate was calculated as (Δ~P)/38 assuming that the respiratory quotient was 1.0, and 38 mol of ATP was produced per 1 mol of glucose. The blood-brain barrier is reported to be impermeable to lactate (24). Thus, the rate of anaerobic glycolysis was calculated from that of lactate accumulation. The rate of ATP production by anaerobic glycolysis was also equal to the rate of lactate accumulation under hypoxia, assuming that all the lactate was produced from glucose.

For conversion of dry weight to wet weight, we determined the wet/dry weight ratio and obtained a value of 4.7. If not specified, "g" in the tables means wet weight.

Evaluation of intracerebral changes in states of hemoglobin and cytochrome oxidase by near infrared spectrophotometry--There has been much recent progress in spectrophotometric analysis using transmitted light in the near infrared region (12-17). This method was applied for measuring the state of oxygenation of hemoglobin and the redox state of cytochrome oxidase in hypoxic mouse brain. Mice were anaesthetized with pentobarbital and fixed in the supine position on a black board. Then, an optical fiber (5mm diameter) was placed over the jaw and the head was illuminated in the ventrodorsal direction. The transmitted light was detected with a photomultiplier detector placed beneath the cranium. The spectral changes induced by hypoxia relative to the spectrum under aerobic conditions were analyzed using a Unisoku

Bio-spectrophotometer, MS-401-01 (Unisoku Co., Ltd. Osaka, Japan) in the wavelength-scanning mode with a scanning time of 10 sec and the interval of 15 sec.

Hypoxic conditions were introduced by covering the whole body of the mouse with a jar, through which mixed gas was passed at a rate of 1.0 l/min. The accuracy of these hypoxic conditions were assessed by the survival time.

Then, we analyzed the changes of hemoglobin and cytochrome oxidase semi-quantitatively. As reported by Hazeki and Tamura (15), the spectral changes at 700-800 nm due to changes in the state of cytochrome oxidase were slight in the brain. Thus, the alteration in the saturation state of cerebral hemoglobin and the total hemoglobin content were calculated from $\Delta A_{700\,nm}$ and $\Delta A_{730\,nm}$ as described by Seiyama et al. (14);

$$\Delta[Hb] = 2.92\,\Delta A_{700\,nm} - 2.75\,\Delta A_{730\,nm}$$

$$\Delta[HbO_2] = -4.23\,\Delta A_{700\,nm} + 5.15\,\Delta A_{730\,nm}$$

$$\Delta[Hb + HbO_2] = -1.31\,\Delta A_{700\,nm} + 2.41\,\Delta A_{730\,nm}$$

The spectral changes at 800-900 nm were the sum of those due to hemoglobin and cytochromes (15). The reduction/oxidation response of cytochrome oxidase (cyt. $\underline{aa_3}$) during hypoxia was calculated from the equation of Hazeki et al. (16),

$$-3.05\,\Delta A_{700\,nm} + 2.66\,\Delta A_{730\,nm} - 1.40\,\Delta A_{830\,nm}$$

Materials--Lactate oxidase was a generous gift from Toyobo Co. (Osaka, Japan). All other enzyme preparations used were products of either Sigma Chemical Co. (U.S.A.) or Boehringer Mannheim (B.R.D.). All reagents were of the highest grade commercially available.

RESULTS

Changes in cerebral lactate and high energy phosphate levels during severe hypoxia--The survival time of experimental animals under hypoxic conditions depends on the partial pressure of O_2 as well as on several other factors, such as the atmospheric temperature and body weight of the animals (25). In our experimental conditions, mice without pretreatment survived at least 30 min under 5.0% O_2, but died after 3.9 ± 0.7 min under 4.4% O_2. During severe hypoxia, cerebral ATP has been shown not to decrease until about one minute before death (26). This was confirmed in the present work. As shown in Fig. 1, under 4.4% O_2, the creatine phosphate level decreased partially in the initial phase, while ATP remained at the control level and lactate accumulated. After 3.0 min, creatine phosphate and ATP decreased rapidly, and at death, the two high energy phosphate compounds had both disappeared and lactate had reached a maximum level.

Fig. 1

Thus, the disappearance of cerebral high energy phosphate compounds seemed to be associated directly with death of hypoxic animals.

Contribution of activated anaerobic glycolysis to ATP supply under severe hypoxia--Under severe hypoxia, anaerobic glycolysis was greatly accelerated in the brain, as indicated by the great accumulation of lactate (Fig. 1). The activation of glycolysis, the Pasteur effect, has been explained as a mechanism for compensating for the shortage of ATP supply resulting from decreased oxidative phosphorylation in ischemia (22) and hypoxia (6). To

estimate the contribution of anaerobic glycolysis to the total ATP supply in the brain under hypoxia, we determined the rate of cerebral energy utilization, which was assumed to be equal to that of ATP production. The metabolic rate of mouse brain was so high that ATP and creatine phosphate vanished within 1 min after decapitation, but total high energy phosphate bonds, including changes in lactate level, decreased linearly for the first 30 seconds (Fig. 2).

Fig. 2

From the slope, the rate was calculated to be 97.3 μmol/g dry weight/min = 20.7 μmol/g wet weight/min for untreated mice. Assuming that the rate of cerebral energy utilization under 4.4% O_2 was equal to that under aerobic conditions, anaerobic ATP synthesis was only 18% of the total amount required, even when glycolysis was accelerated 4.5-fold (TABLE I).

TABLE I

Cerebral anaerobic glycolysis has been observed to be greatly accelerated when the blood glucose level is elevated under ischemia and hypoxia (27). This was also the case in the present study. When hyperglycemic mice, with up to 81.2 mM blood glucose, were exposed to 4.4% O_2, their rate of lactate formation was about 1.4 times that of controls, but their survival time was not significantly prolonged (TABLE I). Assuming that the rate of ATP consumption (Δ~P) in hyperglycemia is the same with that in normoglycemia, anaerobic ATP synthesis increased to meet 25% of the demand. But on 8-fold elevation of the blood glucose level, the increase of anaerobic ATP production from that in normoglycemia amounted to only 7% of the demand. Therefore, it

seemed impossible to prolong the survival time significantly by activation of glycolysis. Indeed, changes in cerebral ATP level were not influenced significantly by increase in glycolysis (data not shown).

Although anaerobic glycolysis contributed only slightly to the cerebral energy demand, it seemed interesting to examine how its activity was increased several-fold immediately after induction of hypoxia. Little change was observed in the level of fructose-2,6-bisphosphate, a potent activator of fructose-6-phosphate kinase, but the cyclic AMP level increased several-fold under hypoxia, indicating involvement of protein phosphorylation in the initiation of the Pasteur effect in the brain (TABLE II).

TABLE II

Effect of pentobarbital anaesthesia--Hypoxic attack is known to be effectively alleviated by anesthesia. Pentobarbital anesthesia is reported to reduce the demands for ATP ($\Delta\sim P$) and oxygen (28). Actually, in our conditions of anaesthesia, the rate of consumption of ~P was significantly reduced to 75% of that in untreated mice (Fig. 2), and the survival time under 4.4% O_2 was increased more than 2-fold (TABLE I). The cerebral ATP level changed little until about 2 min before death, as observed in the case of untreated animals (TABLE III).

TABLE III

In anesthetized mice, acceleration of anaerobic glycolysis was significantly less than in controls, and its contribution to the total synthesis of ATP was about 13%. Thus, pentobarbital anaesthesia probably prolonged the survival time of mice by causing continuance of oxidative phosphorylation, which supported 87% of

the energy demand. However, in the late phase, the supply could no longer meet the demand because of the limited supply of O_2 to the brain under hypoxia at 4.4% O_2.

Changes in the oxygenation state of cerebral hemoglobin and redox state of cytochrome oxidase after induction to hypoxia-- Since decrease in the cerebral ATP level in the late phase of severe hypoxia was probably caused mainly by an insufficient energy supply from the oxidative phosphorylation system, we examined the changes in the redox state in pentobarbital-anesthetized mice by the near infrared spectrophotometric method. Fig. 3 shows typical results on spectral changes from the time of induction of hypoxia until death at 12.7 min.

Fig. 3

The spectrum obtained 15 sec after induction to hypoxia indicated predominantly deoxygenation of hemoglobin and a slight reduction of cytochrome oxidase, judged from the blue shift of the intersecting point from the isosbestic point at 805 nm. Then deoxygenation of hemoglobin proceeded and was almost complete at 2.5 min. During this period, reduction of cytochrome oxidase also proceeded, as judged from the further blue shift of the intersecting point and decrease in absorbance between 800 and 860 nm (Fig. 3a). From 2.5 min to 5min, the intersecting point shifted gradually to longer wavelengths, indicating increase in the total amount of hemoglobin due to increase in cerebral blood volume (Fig. 3b). Subsequently little change was observed except for decrease in absorbance at about 830 nm, probably due to further gradual reduction of cytochrome oxidase (Fig. 3c). After death, the spectra moved in parallel to shorter wavelengths in-

dicating decrease in blood volume and complete reduction of cytochrome oxidase (Fig. 3d). From the series of spectra, the changes in oxygenation state of cerebral hemoglobin were calculated by the formula of Seiyama et al.(14), and are plotted in Fig. 4.

Fig. 4

The plots show the changes in oxygenation state of hemoglobin a little more precisely, but the pattern is approximately the same as that described above. The maximum level of deoxygenated hemoglobin, which was reached in the middle phase of hypoxia, seemed to represent the state of full deoxygenation, because the spectral changes do not reflect the arterial but predominantly the venous phase (14). Fig. 4 also shows changes in the total amount of hemoglobin, which was calculated from the sum of the changes of deoxy- and oxyhemoglobin (14). The curve represents change in cerebral venous blood volume.

The spectral change corresponding to the redox state of cytochrome oxidase was calculated by the formula of Hazeki et al. (16). Reduction of cytochrome oxidase proceeded in the first 2.5 min, followed by slow reoxidation until about 5 min, probably due to slight increase in the oxygen supply. Then the cytochrome was again reduced and its reduction continued more slowly until death, indicating gradual decrease in the oxygen supply. The slight reduction observed after death, may indicate complete reduction due to cut-off of the oxygen supply (Fig. 5).

Fig. 5

DISCUSSION

In the brain, glucose is the sole substrate for production of ATP. Under aerobic conditions, glucose is oxidized almost completely to carbon dioxide and water, whereas in hypoxia or ischemia, lactate accumulates due to acceleration of glycolysis (29). In the present study, we analyzed the changes in levels of compounds that are related to energy metabolism under severe hypoxia and found that oxidative phosphorylation is essential for ATP supply and that its shortage due to hypoxia cannot be compensated for fully by anaerobic glycolysis, even in hyperglycemia. Lowry et al. (20) reported that in complete ischemia, in spite of 7-fold acceleration of glycolysis, ATP synthesis by anaerobic glycolysis could meet only 29% of the demand, and that the cerebral levels of ATP and creatine phosphate were depleted within about 1 min. In our conditions under 4.4% O_2, the ATP level was maintained for 3 min until about 1 min before death. In these conditions, 3.5-fold increase of glycolysis was observed, but anaerobic ATP production met only about 20% of the demand. Thus, the remainder must have been supplied by oxidative phosphorylation, the activity of which decreased gradually in the late phase of hypoxia due to decrease in oxygen supply from the blood and finally became unable to meet the energy demand. The rate of ATP utilization in the brain is so high that slight imbalance due to shortage of its supply probably caused rapid decrease in the cellular ATP level. From our results, this shortage of supply could be accounted for by progressive reduction of cytochrome oxidase, or in other words, decrease of tissue

oxygen.

Since the pioneering work by Jobsis (12) and its development in Tamura's laboratory, analysis of transmitted light in the near infrared region (700-900nm) has been used to study changes in the state of intracerebral hemoglobin and cytochrome oxidase in rat brain (13,15-17). Using this method, we observed that in mouse brain cerebral hemoglobin was quickly deoxygenated after induction of hypoxia, and was soon deoxygenated completely in venous blood. The method used did not provide any information on changes in the oxygenation state of hemoglobin in arterial blood (14). Direct analysis of blood gas of SD rats revealed that the arterial oxygen tension decreased rapidly from 120 mmHg to 23 mmHg when the O_2 level was reduced to 4.4%, but that this level of oxygenated hemoglobin was then maintained until death (H. Ueda, unpublished data). We could not measure the arterial oxygen tension of mice, but it probably showed a very similar change under 4.4% O_2. Thus, under 4.4% O_2 the oxygen carried in arterial blood have been less than a quarter of that in normoxia, and was probably used up in hypoxic brain.

Monitoring of the redox state of cytochrome oxidase was a little more difficult than that of the oxygenation state of hemoglobin, because the infrared peak of its oxidized form is broad (30) and spectral changes were affected by changes in deoxygenation of hemoglobin and in blood volume. In hypoxic mouse brain, cytochrome was observed to be reduced very slowly in the middle phase of hypoxia and to be almost completely reduced at death, implying a gradual decrease in the oxygen supply during the middle phase of hypoxia. This was very curious because in

this phase of hypoxia the oxygen tensions in the artery and vein were unchanged. The discrepancy between changes in blood oxygen tension and the redox state of cytochrome may be explained by decrease in cerebral blood flow. Actually, decrease in the arterial CO_2 pressure during severe hypoxia is reported to have adverse effects on the blood pressure (2,31). However, the mechanism of decrease in oxygen supply in the late phase of hypoxia is still controversial and requires study.

We thank Ms. K. Chihara for technical assistance.

REFERENCES

1. Gurdjian, E. S., Stone, W. E., & Webster, M. J. E. (1944) Arch. Neurol. Psychiat. **54**, 472-477
2. Siesjo, B. K. & Nilsson, L. (1971) Scand. J. Clin. Lab. Invest. **27**, 83-96
3. Kogure, K., Scheinberg, P., Utsunomiya, Y., Kishikawa, H., & Busto, R. (1977) Ann. Neurol. **2**, 304-310
4. Duffy, T. E., Nelson, S. R., & Lowry, O. H. (1972) J. Neurochem. **19**, 959-977
5. Kogure, K., Busto, R., Scheinberg, P., & Reinmuth, O. (1975) J. Neurochem. **24**, 471-478
6. Cohen, P. J., Alexander, S. C., Smith, T. C., Reivich, M., & Wollman, H. (1967) J. Appl. Physiol. **23**, 183-189
7. Norberg, K. and Siesjo, B. K. (1975) Brain Res. **86**, 31-44
8. Kogure, K., Scheinberg, P., Reinmuth, O. M., Fujishima, M., & Busto, R. (1970) J. Appl. Physiol. **29**, 223-229
9. Johannsson, H. & Siesjo, B. K. (1975) Acta. Physiol. Scand. **93**, 269-276
10. Borgstrom, L., Johannsson, H., & Siesjo, B. K. (1975) Acta Physiol. Scand. **93**, 423-432
11. Kerr, S. E. (1942) J. Biol. Chem. **145**, 647-656
12. Jobsis, F. F. (1977) Science **198**, 1264-1267
13. Wiernsperger, N. Sylvia, A. L., & Jobsis, F. F. (1981) Stroke **12**, 864-868
14. Seiyama, A., Hazeki, O., & Tamura, M. J. Biochem. (1987) in press
15. Hazeki, O. & Tamura, M. J. Appl. Physiol. (1988) in press

16. Hazeki, O., Seiyama, A., & Tamura, M. (1987) in Oxygen Transport to Tissue IX (Silver, I. A. & Silver A., eds) pp.283-289, Plenum Press, New York

17. Kariman, K. & Burhart, D. S. (1985) Biochem. Biophys. Res. Commun. **126**, 1022-1028

18. Ponten, U., Ratcheson, R. A., & Siesjo, B. K. (1973) J. Neurochem. **21**, 1121-1126

19. Watanabe, F., Hashimoto, T., & Tagawa, K. (1985) J. Biochem. **97**, 1229-1234

20. Furuya, E., Hotta, K., & Tagawa, K. (1986) Biochem. Biophys. Res. Comm. **141**, 931-936

21. Uyeda, K., Furuya, E., Richards, C. S., & Yokoyama, M. (1982) Mol. Cell. Biochem. **48**, 97-120

22. Lowry, O. H., Passonneau, J. V., Hasselberger, F. X., & Schulz, D. W. (1964) J. Biol. Chem. **239**, 18-30

23. Levy, D. E. & Duffy, T. E. (1975) J. Neurochem. **24**, 1287-1289

24. Oldendorf, W. H. (1972) Eur. Neurol. **6**, 49-55

25. Britton, S. W. & Kline, R. F. (1945) Am. J. Physiol. **145**,190-202

26. Holowach-Thurston, J., Hauhart, R. E., & Jones, E. M. (1974) Pediatr. Res. **8**, 238-243

27. Plum, F. (1983) Neurology **33**, 222-233

28. Piatt, J. H. Jr. & Schiff, S. J. (1984) Neurosurgery **15**, 427-444

29. Hawkins, R. A. & Mans, A. M. (1983) in Handbook of Neurochemistry Vol. 3. Metabolism in the nervous system (Lajtha A. ed), pp. 259-294. Plenum Press, New York

30. Griffith, D.E. & Wharton D. C. (1961) J. Biol. Chem. 236, 1850-1856

31. Gottesfeld, Z. & Miller, A. T. (1969) Am. J. Physiol. 216, 1374-1379

TABLE I. Glycolytic rates and contribution of anaerobic glycolysis to ATP demand in mouse brain under 4.4% O_2. Values are means (± SD) for six mice. Data in parentheses show percentages of the demand (20.7 μmol/g·min with no anaesthetic, 15.3 μmol/g·min with pentobarbital; see also Fig. 2). The mean blood glucose levels were 11.2 mM in un-treated mice, 81.2 mM in hyperglycemic mice, and 14.1 mM in pentobarbital-treated mice.

	Survival Time	Anaerobic ATP Production[a]	Glycolysis		
			Aerobic[b]	Anaerobic[c]	Sum
	(min)	(μmol ~P/g·min)	(μmol/g·min)		
No anaesthetic					
Normoxia	--	0.0	0.54	0.0	0.54
Hypoxia	3.9 ± 0.7	3.72 ± 0.86 (18%)	0.45	1.86	2.31
Hypoxia +Hyperglycemia	4.0 ± 0.7	5.20 ± 0.98 (25%)	0.41	2.60	3.01
Pentobarbital					
Normoxia	--	0.0	0.40	0.0	0.40
Hypoxia	9.1 ± 2.6	2.03 ± 0.58 (13%)	0.35	1.02	1.37

[a](Anaerobic ATP production) = (Δ Lactate)/(survival time).

[b](Rate of aerobic glycolysis) = (Δ~P - Δ Lactate)/38.

[c](Rate of anaerobic glycolysis) = (Δ Lactate)/2.

TABLE II. Cerebral levels of modulators of glycolysis after induction to hypoxia. Brains were frozen 1 min after induction of hypoxia (4.4% O_2). Values were means ± SD for 3 mice. (*P<0.05, vs. Normoxia)

	cyclic AMP	Fructose-2,6-bisphosphate
Normoxia	9.1 ± 1.8	46.5 ± 6.1
Hypoxia	17.9 ± 3.6*	43.6 ± 3.9
Hypoxia + Hyperglycemia	16.8 ± 0.2*	42.0 ± 2.2

(nmol/g dry weight)

TABLE III. Levels of high energy phosphate compounds in brains of pentobarbital anesthetized mice under 4.4% O_2. At the indicated times, the brains were frozen and the levels of metabolites were analyzed as described in "MATERIALS AND METHODS". Values are means ± SD for at least three brains.

	Alive			Dead[a]
	0 min	4 min	7 min	(6-14 min)
ATP	10.9 ± 0.9	10.1 ± 0.5	10.4 ± 0.6	1.3 ± 0.5
P-Cr	19.9 ± 2.0	12.1 ± 4.7	12.0 ± 5.8	0.6 ± 0.4

(μmol/g dry weight)

[a]Mouse brains were frozen immediately after death.

Legends to figures

Fig. 1. Changes in cerebral levels of high energy phosphate compounds (A), glucose and lactate (B) under 4.4% O_2. At the times indicated, brains were frozen and the levels of compounds were measured as described in "MATERIALS AND METHODS". (A) Creatine phosphate (P-Cr, ●-●), ATP (▲-▲), ADP (■-■), AMP (▼-▼) (B) lactate (●-●), glucose (▼-▼). Points are mean values for at least three animals, and vertical bars represent SDs (not shown when less than the diameter of the symbol). *P<0.05, **P<0.01 vs. control.

Fig. 2. Changes in the contents of total high energy phosphate bond (Σ(~P) = PCr + 2 x ATP + ADP -Lactate) after decapitation of unanesthetized (○-○) and pentobarbital-anesthetized (●-●) mice. Points are mean values for three (or two) mice, and vertical bars represent SDs. The rate of energy utilization was calculated from the slope.

Fig. 3. Spectral changes of light transmitted through mouse brain during hypoxia. (a) 0-2.5 min, (b) 2.5-5.0 min, (c) 5.0-11.25 min, (d) 11.25-13.5 min.

Fig. 4. Changes in oxygenation state of hemoglobin in mouse brain. Values were calculated as reported by Seiyama et al.(14).

Fig. 5. Change in redox state of cytochrome oxidase in mouse brain. Values were calculated as reported by Hazeki et al.(16).

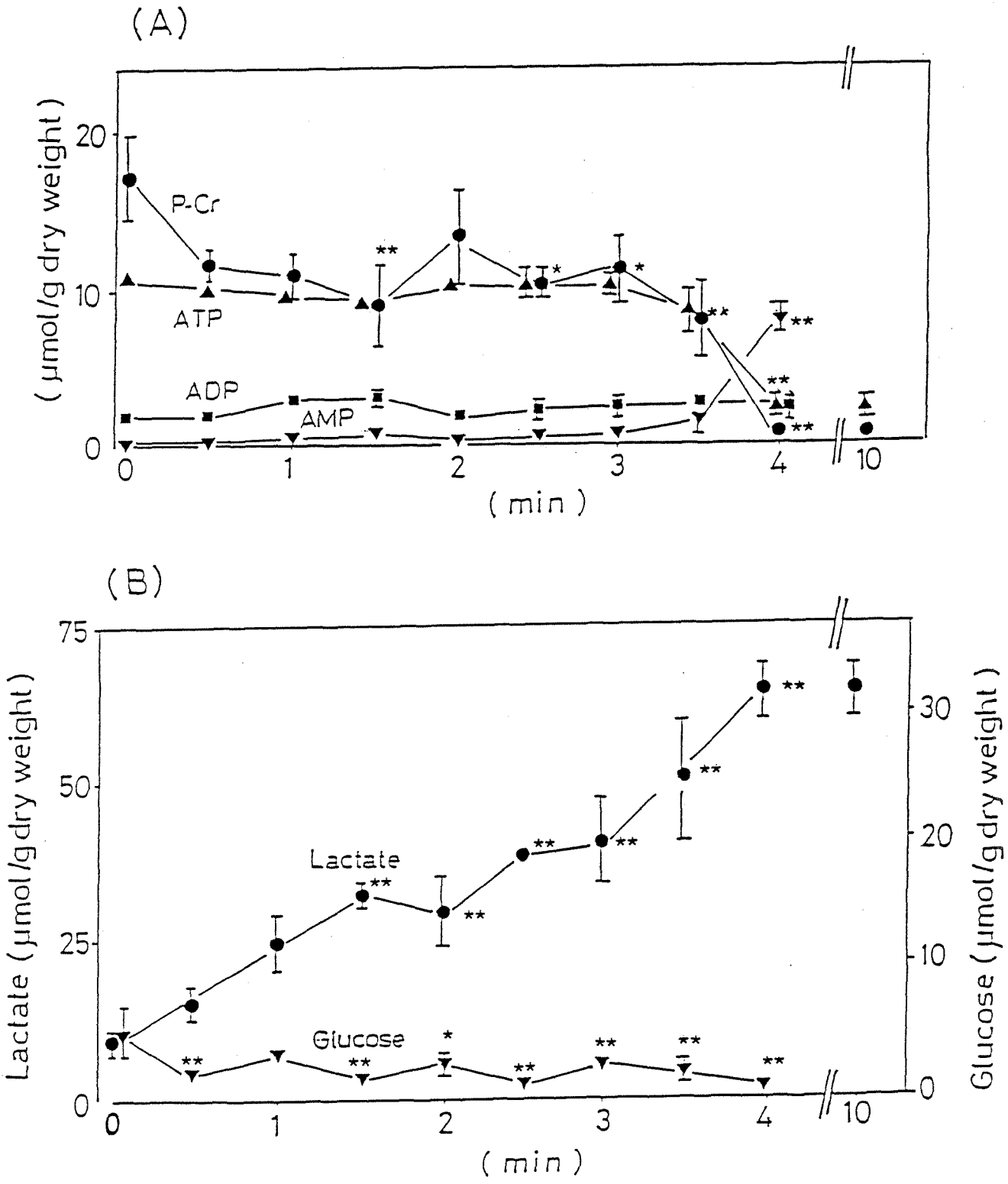

Fig. 1. H. Ueda et al.

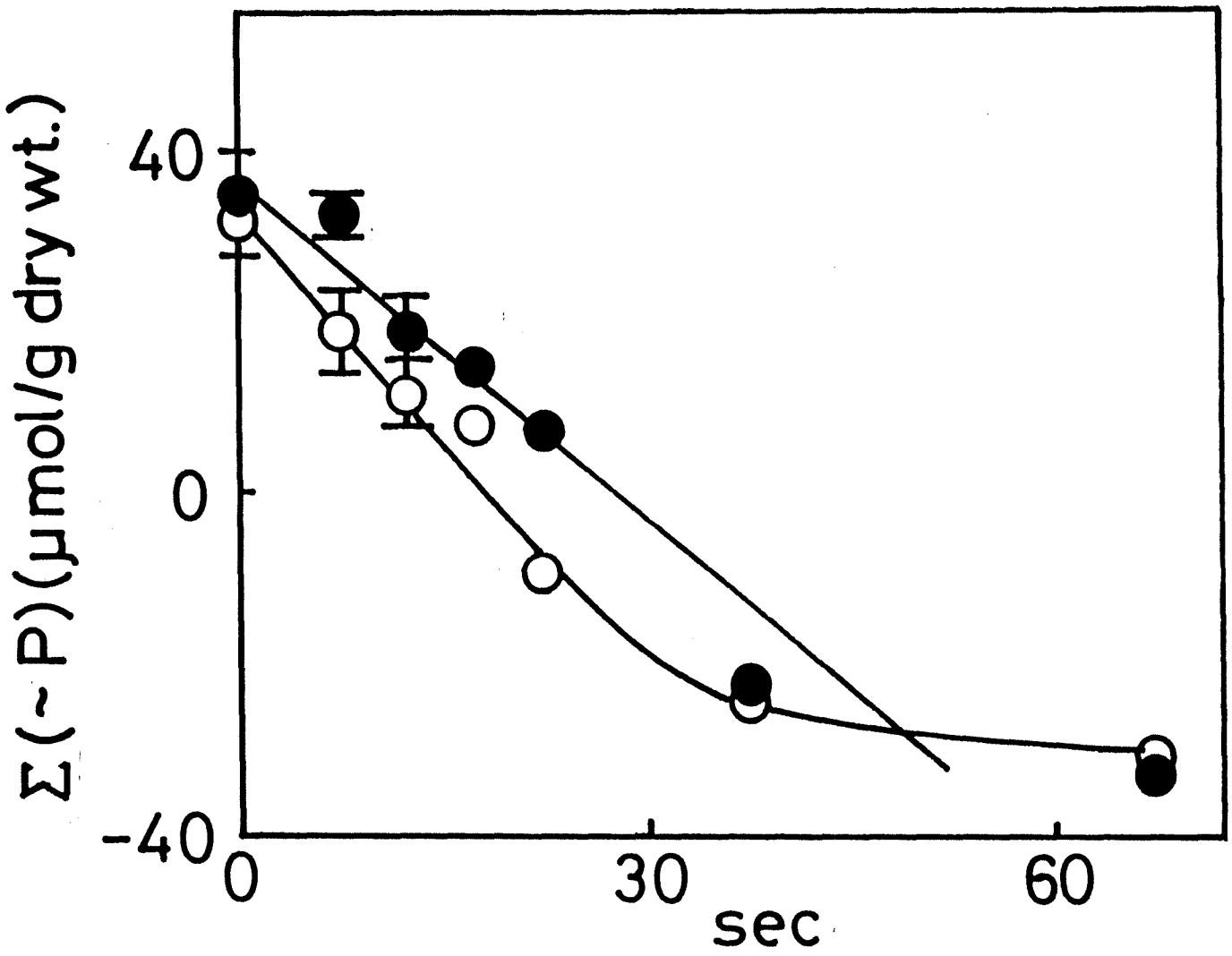

Fig. 2. H. Ueda et al.

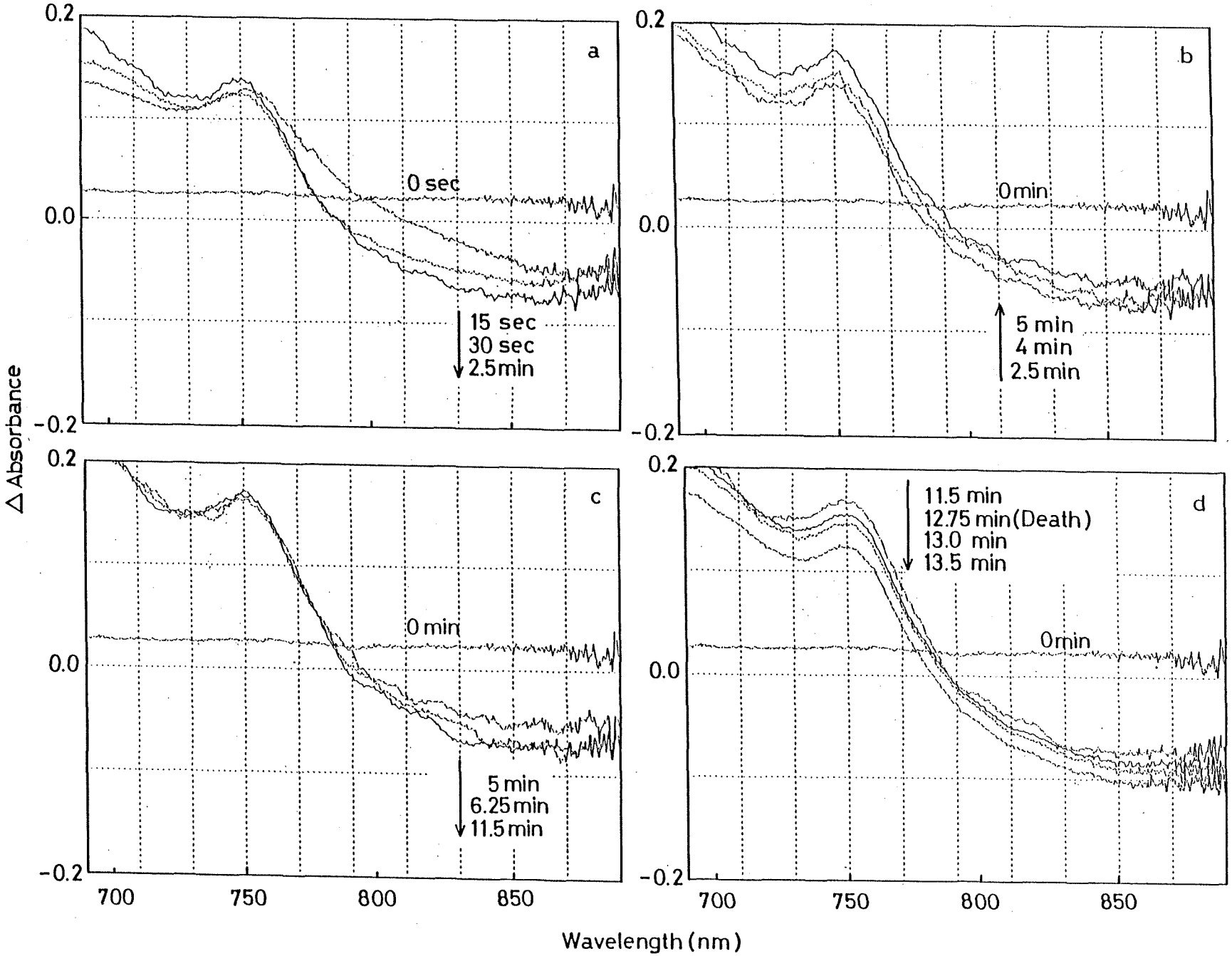

Fig. 3. H. Ueda et al.

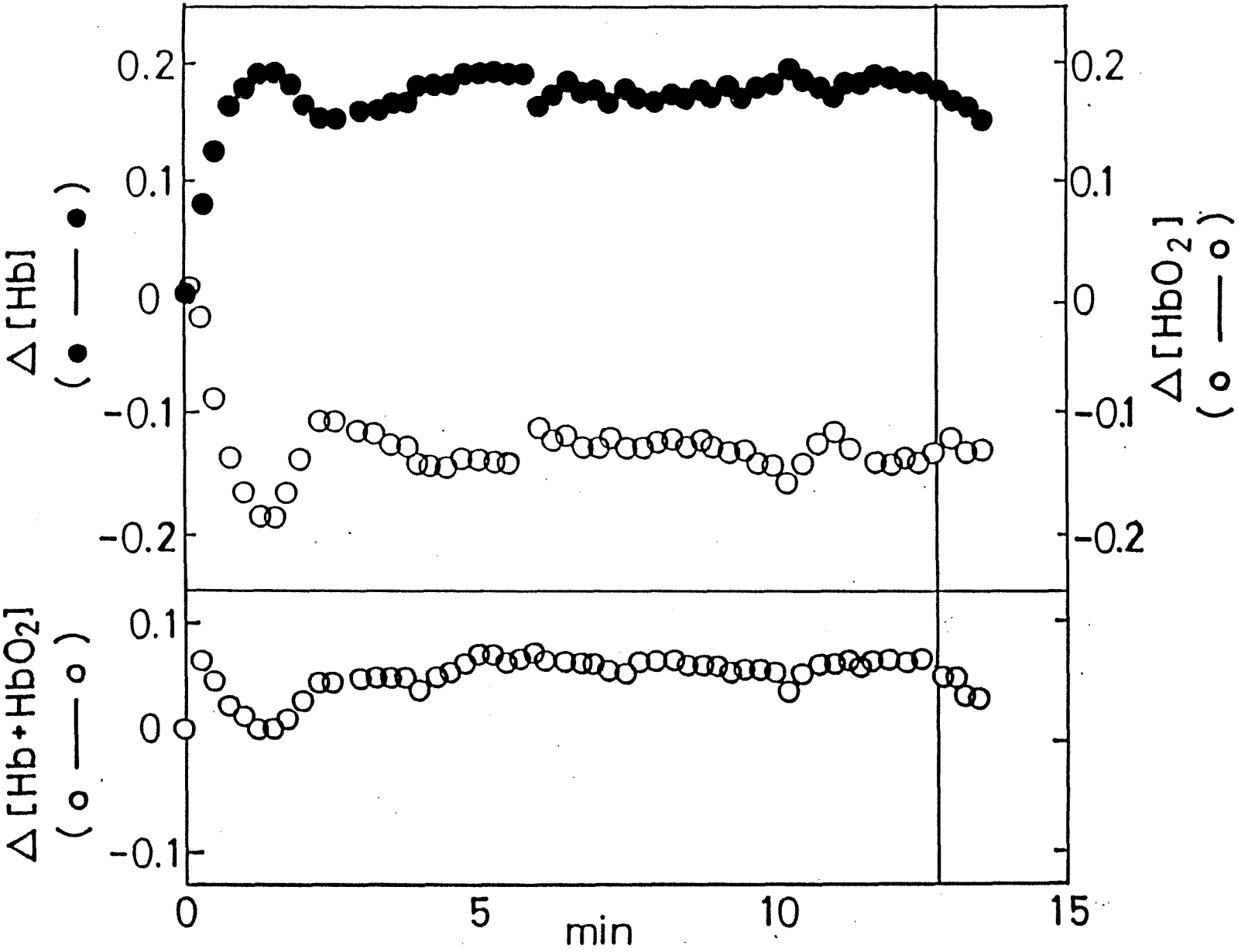

Fig. 4 H. Ueda et al.

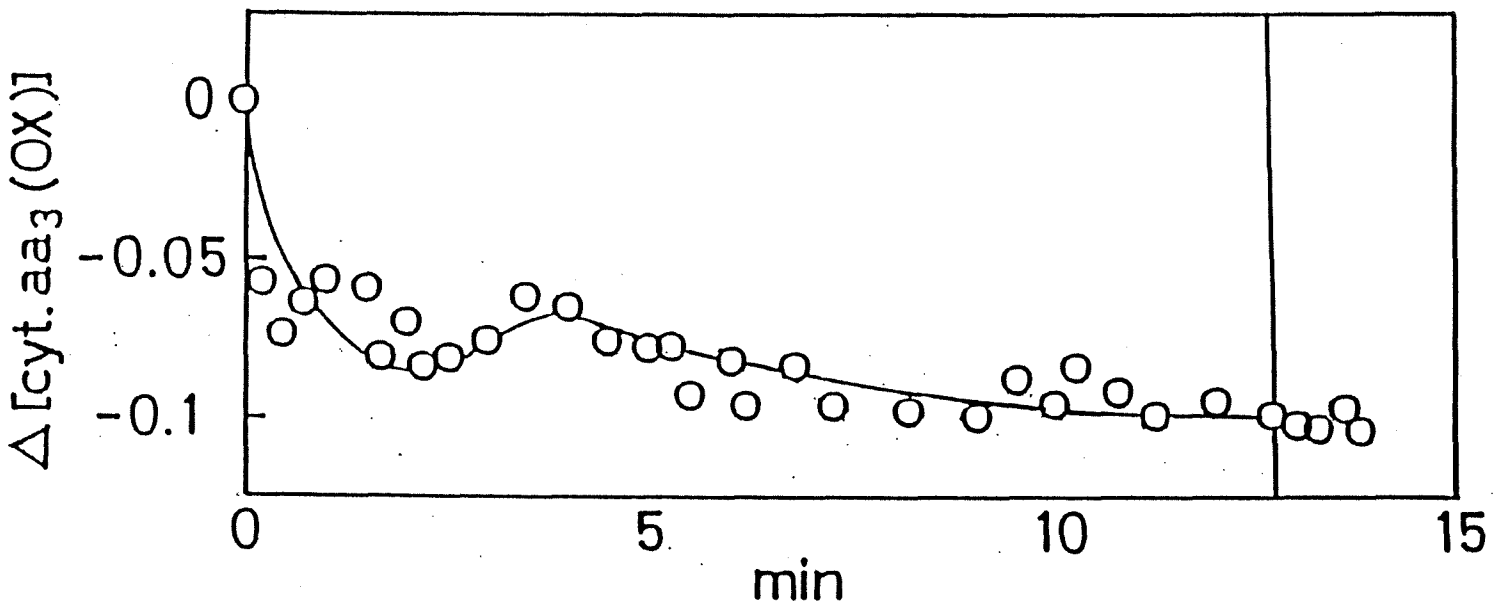

Fig. 5. H. Ueda et al.

Japanese Journal of Physiology, **37**, 411–423, 1987

^{31}P NMR Studies on the Isolated Perfused Mandibular Gland of the Rat

Masataka MURAKAMI, Yoshiteru SEO, Hiroshi WATARI, Hirokazu UEDA,* Tadao HASHIMOTO,* and Kunio TAGAWA*

Department of Molecular Physiology, National Institute for Physiological Sciences, Okazaki, 444 Japan

Japanese Journal of Physiology, **37**, 411–423, 1987

^{31}P NMR Studies on the Isolated Perfused Mandibular Gland of the Rat

Masataka MURAKAMI, Yoshiteru SEO, Hiroshi WATARI, Hirokazu UEDA,* Tadao HASHIMOTO,* and Kunio TAGAWA*

Department of Molecular Physiology, National Institute for Physiological Sciences, Okazaki, 444 Japan
** Department of Physiological Chemistry, Medical School, Osaka University, Kita-ku, Osaka, 530 Japan*

Abstract Phosphorus nuclear magnetic resonance (^{31}P NMR) was used to study energy metabolism in the rat mandibular gland. The gland was isolated, perfused arterially and set in the NMR tube. At rest, 7 resonance peaks were observed and 6 peaks identified from low field as: 1) sugar phosphates (SP) and nucleotide monophosphate (NMP), 2) inorganic phosphate (Pi), 3) creatine phosphate (PCr), 4) γ-nucleotide triphosphate (NTP) and β-nucleotide diphosphate (NDP), 5) α-NTP, α-NDP, NAD^+, and NADH, 6) an unknown peak, and 7) β-NTP. From the results of high performance liquid chromatography (HPLC), NTP consisted mainly of ATP and GTP, and UTP was not detected. The tissue contents of ATP and GTP in the perfused gland were determined by HPLC as 1.86 ± 0.03 and 0.37 ± 0.01 mmol/kg wet tissue (S.E., $n=5$). From ^{31}P NMR and HPLC data, the tissue levels of creatine phosphate, ADP, and sugar phosphates were estimated as 3.3, 0.4, and 4.2 mmol/kg wet tissue, respectively. The cessation of perfusion decreased the tissue levels of PCr and ATP and increased those of Pi and SP. On the other hand, administration of acetylcholine (1 μM), which is an optimal dose for secretion, decreased PCr and increased Pi but did not change SP. The ATP was unchanged initially and slowly decreased to the lower level during sustained secretion. These findings suggest that a sustained secretion requires more energy from ATP hydrolysis rather than initial secretion.

Key words: ^{31}P NMR, perfused salivary gland, creatine phosphate, ATP, GTP.

Fluid secretion by the salivary gland is considered to be an osmotic flow induced by the active transport of electrolytes and is accompanied by an increase in energy metabolism. Oxygen consumption (TERROUX and BURGEN, 1959; STEWART *et*

Received for publication January 27, 1987

al., 1983), heat production (MURAKAMI, 1979), and lactate production (NORTHUP, 1935) increased several times during secretion. But these parameters deal with only the overall results of metabolism.

Phosphorus nuclear magnetic resonance (^{31}P NMR) spectroscopy enabled a sequential and non-invasive measurement of the phosphorus compounds in the same organ. Because of these advantages, ^{31}P NMR has already been applied to various organs such as the heart (HOLLIS *et al.*, 1978) and the liver (MCLAUGHLIN *et al.*, 1979). We applied NMR to the perfused submandibular gland of the dog (MURAKAMI *et al.*, 1983, 1984; NAKAHARI *et al.*, 1985) and reported that creatine phosphate and ATP decreased by acetylcholine. However, several problems remain unsolved if the method is applied to the canine gland: 1) the difficulty of surgical operation, 2) the large variation in the arterial routes to the gland, 3) the unsuitable size of the gland for the conventional NMR probe (less than 15 mm in diameter), etc. To overcome these problems, we have developed a procedure to perfuse the rat mandibular gland in an NMR tube (10 mm in diameter).

The present study demonstrates the application of the ^{31}P NMR method to the perfused mandibular gland of the rat. We assigned the spectral peaks to nucleotide phosphates by authentic samples, and confirmed them by using a high performance liquid chromatography (HPLC). To assess the energy state during sustained secretion, we measured the levels of ATP, creatine phosphate (PCr), and inorganic phosphate (Pi) sequentially during prolonged stimulation with acetylcholine (ACh) (1 μM) for 1 h.

METHODS

Perfusion. Male rats (Std: Wistar, 280–350 g weight) were used. The animals were anesthetized by an intraperitoneal injection of pentobarbital sodium (Nembutal®, 50–70 mg/kg body weight). The mandibular glands, weighing 150–290 mg, were surgically isolated for perfusion as described elsewhere (CASE *et al.*, 1980; COMPTON *et al.*, 1981) and placed in a 10-mm diameter NMR tube. The mandibular artery was cannulated with a polyethylene tube that was pulled over a flame. Vascular perfusion of the gland offers two advantages: 1) a sufficient oxygen supply via capillary bed; 2) a rapid replacement of extracellular fluid.

The gland was perfused arterially with the aid of a Cole-Palmer® peristaltic pump at the rate of 2 ml/min. The composition of the control perfusate (in mM) was as follows: Na 146.0, K 4.3, Ca 1.0, Mg 1.0, Cl 148.3, phosphate 1.0, and glucose 5.0. The solution was buffered at pH 7.4 with HEPES (N-2-hydroxyethylpiperazine-N′-2-ethanesulfonic acid) (10 mM) and gassed with 100% O_2. The temperature of the experiment was kept at 24°C.

^{31}P NMR. A superconducting magnet of 8.45 T (Oxford) was used and ^{31}P NMR spectra were collected at 145.8 MHz using a WM-360wb NMR spectrometer (Bruker). For the kinetic measurement, radio frequency (RF) pulses of 5 or 10 μs (15 or 30° pulse) followed by a relaxation delay (RD) of 0.3 s and 1,000-times

accumulation were taken (5 min for each spectrum). Since RD of the kinetic measurement was too short for complete relaxation, we cannot relate the signal intensities among different kinds of phosphorus compounds. However, we can increase a time resolution, and the time course of each phosphorus compound can be traced. For determination of the relative concentrations of the phosphorus compounds in the gland, a pulse width of 5 μs, a RD of 4.0 s and 512-times accumulation were taken (35 min for each spectrum). The resonance areas beneath the phosphorus compounds were measured for quantitative analysis. Tissue concentrations of phosphorus compounds were obtained by comparison of the relative concentrations with the value of ATP content determined by HPLC.

Chemical analysis of nucleotides by HPLC. The procedure for analysis of ATP was according to the method of WATANABE *et al.* (1985). Immediately after the control perfusion for 20 min, or without perfusion, the glands were dissected and frozen with a brass clamp. The brass clamp was cooled in liquid nitrogen before use. The frozen samples were freeze-dried and extracted with perchloric acid (0.5 N). The extract was neutralized at pH 7 with 9.2 N KOH and analyzed by HPLC (Hitachi 638) with an anion exchange column (TSK, DEAE-2SW). The column was eluted with 0.25 M sodium phosphate (pH 6.2) at the rate of 1.0 ml/min, and the nucleotides were detected at 260 nm.

RESULTS

Identification of ^{31}P NMR resonances

Seven resonance peaks were observed in the ^{31}P NMR spectrum of the rat mandibular gland (Fig. 1). By comparing them with spectra of the authentic samples, 6 peaks were identified as: 1) sugar phosphates (SP) and nucleotide monophosphate (NMP), 2) inorganic phosphate (Pi), 3) creatine phosphate (PCr), 4) γ-nucleotide triphosphate (NTP) and β-nucleotide diphosphate (NDP), 5) α-NTP, α-NDP, NAD^+, and NADH, 6) an unknown peak, and 7) β-NTP. This assignment agreed with reported spectra (HOULT *et al.*, 1974; BURT *et al.*, 1976; NAVON *et al.*, 1977). The areas and the heights of phosphorus peaks were stable during the perfusion with the control solution for 24 h, indicating that the viability of the gland can be maintained for 24 h.

Chamical analysis of nucleotides by HPLC

Figure 2 shows a typical chromatogram of nucleotides extracted from the rat mandibular gland, which was perfused arterially for 20 min before freezing. By comparison with the chromatogram of authentic samples, 6 peaks were assigned to: 1) GMP (guanosine 5′-phosphate), 2) AMP (adenosine 5′-phosphate), 3) GDP (guanosine 5′-diphosphate), 4) ADP (adenosine 5′-diphosphate), 5) GTP (guanosine 5′-triphosphate), and 6) ATP (adenosine 5′-triphosphate). The uridine nucleotides such as UDP and UTP, and the cytidine nucleotides were not detected.

The tissue concentrations of ATP, ADP, and AMP in the perfused gland were

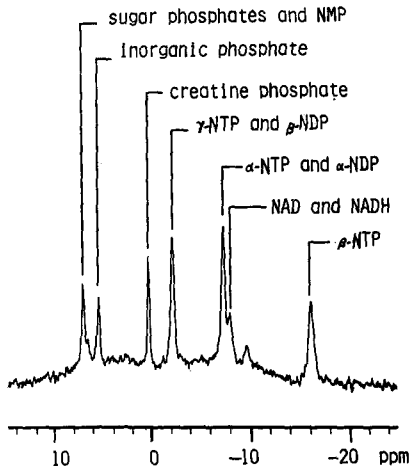

Fig. 1. Assignment of ^{31}P NMR spectrum of perfused mandibular gland of the rat. Seven resonance peaks were observed and 6 peaks were identified as: 1) sugar phosphates (SP) and nucleotide monophosphate (NMP), 2) inorganic phosphate (Pi), 3) creatine phosphate (PCr), 4) γ-nucleotide triphosphate (NTP) and β-nucleotide diphosphate (NDP), 5) α-NTP, α-NDP, NAD^+, and NADH, 6) an unknown peak, and 7) β-NTP.

Table 1. Tissue concentrations of Nucleotides in the mandibular gland of rat; measured by HPLC (mmol/kg wet weight).

	ATP	ADP	AMP	GTP	GDP	GMP
1) perfused	1.86	0.47	0.23	0.37	0.10	0.40
($n=5$)	$\pm$0.03	$\pm$0.02	$\pm$0.01	$\pm$0.01	$\pm$0.004	$\pm$0.02
2) *in situ*	1.65	0.63	0.37	0.30	0.12	0.40
($n=5$)	$\pm$0.05*	$\pm$0.01**	$\pm$0.03*	$\pm$0.01**	$\pm$0.004***	$\pm$0.006$^{N.S.}$

Values are mean $\pm$ S.E. for No. of glands given in parentheses. *,**,*** and $^{N.S.}$ denote significant difference; $p<0.01$, $p<0.001$, $p<0.02$ and "no significant difference."

	ATP/ΣNTP	ADP/ΣNDP	AMP/ΣNMP
1) perfused	0.835	0.818	0.367
2) *in situ*	0.845	0.838	0.479

$\Sigma NTP = ATP + GTP$, $\Sigma NDP = ADP + GDP$, $\Sigma NMP = AMP + GMP$.

measured as 1.86, 0.47, and 0.23 mmol/kg wet weight, respectively (Table 1). The tissue concentrations of GTP, GDP, and GMP were 0.37, 0.10, and 0.40 mmol/kg wet weight, respectively. Since nucleotides other than adenine were not observed, the ratio of ATP to total NTP, ATP/NTP = ATP/(ATP + GTP), was 0.84,

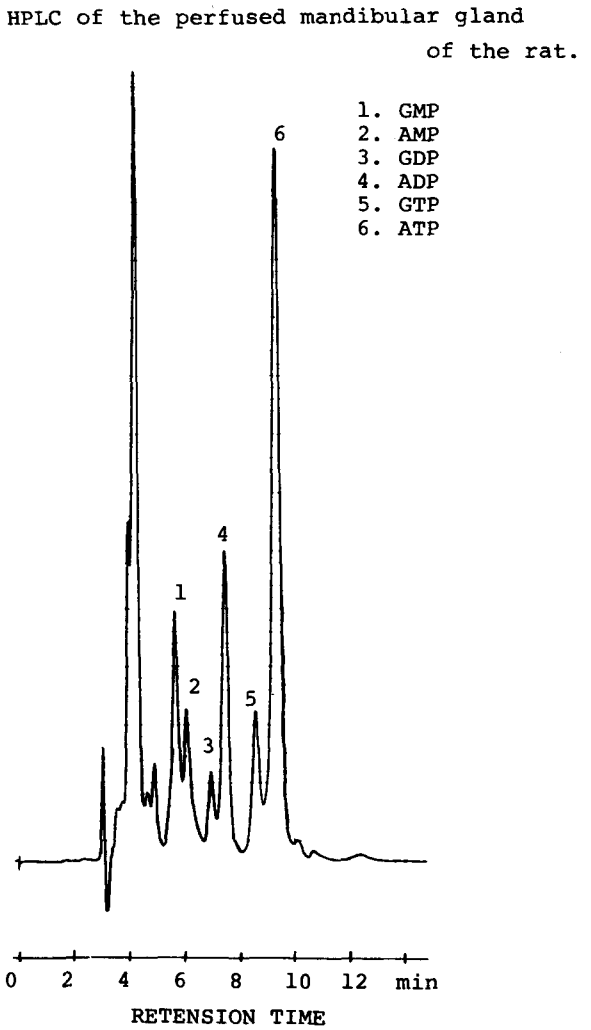

Fig. 2. HPLC chromatogram of nucleotides extracted from the rat mandibular gland, which was perfused for 20 min before dissection. By comparison with the chromatogram of authentic samples, 6 peaks were assigned to: 1) GMP, 2) AMP, 3) GDP, 4) ADP, 5) GTP, and 6) ATP.

ADP/NDP was 0.82, and AMP/NMP was 0.37.

Table 1 also shows the comparison of the nucleotide levels between a perfused gland and an *in situ* gland, which was frozen immediately without perfusion. The ATP and GTP levels of the perfused gland were slightly higher than those of the *in situ* gland. The ADP and AMP levels of the perfused gland were less than those of the *in situ* gland. The total adenine nucleotide (sum of ATP, ADP, and AMP) in the perfused gland was the same as in the *in situ* gland. These observations could be interpreted as: 1) the O_2 supply to the *in situ* gland could be decreased by the

lowered respiration and circulation under deep anesthesia; 2) the lower temperature (24°C) could slow ATP hydrolysis in the perfused gland. The GDP of the perfused gland was slightly less than that of the *in situ* gland. The GMP levels of both glands were similar.

The two glands were left uncirculated for about 20 min (hypoxic gland), thereafter frozen, and their nucleotide levels were measured by an HPLC. The ATP content of the hypoxic gland was about 40% less than that of the perfused gland. The ADP and AMP levels were both higher than those of the perfused gland. The total content of adenine nucleotide (sum of ATP, ADP, and AMP) in the perfused gland was larger than in the hypoxic gland.

Resting levels of phosphorus compounds estimated from ^{31}P NMR spectra and HPLC data

The proportion of the resonance areas in the ^{31}P NMR spectrum reflected the proportion of the amounts of phosphorus compounds included in the observable space of the NMR tube under the condition that all phosphorus spins were completely relaxed during the relaxation delay of the measurement. Table 2 shows the relative concentrations of phosphorus measured from the quantitative ^{31}P NMR spectra. The proportion of NTP : NDP : PCr : Pi : SP+NMP was 1 : 0.23 : 1.50 : 1.60 : 1.87. Accordingly, the resting levels of PCr, ADP, Pi, and SP+NMP were estimated as 3.3, 0.4, 3.6, and 4.2 mmol/kg wet weight, using the above-mentioned ATP value measured by HPLC.

Table 2. Relative concentration of phosphorus compounds measured by ^{31}P-NMR spectroscopy, and the tissue concentrations estimated from NMR spectra and ATP and GTP levels (HPLC data in Table 1).

Relative concentrations of phosphorus compounds estimated from ^{31}P-NMR spectra

SP+NMR	Pi	PCr	NDP	NAD^++NADH	NTP
1.87±0.08 (26)	1.60±0.08 (26)	1.50±0.11 (26)	0.23±0.06 (26)	0.78±0.05 (26)	1

SP (sugar phosphates), Pi (inorganic phosphate), PCr (creatine phosphate), NMP=AMP+GMP, NDP=ADP+GDP, NTP=ATP+GTP. Values are mean±S.E. for No. of glands given in parentheses.

Tissue concentrations of phosphorus compounds (mmol/kg wet weight)

SP+NMP	Pi	PCr	NDP	(ADP)	NAD^++NADH	NTP	(ATP)
4.2	3.6	3.3	0.5	(0.4)	1.7	2.2*	(1.86*)

* Values of NTP and ATP were measured by HPLC and values of other phosphorus compounds were estimated from relative concentrations and NTP value.

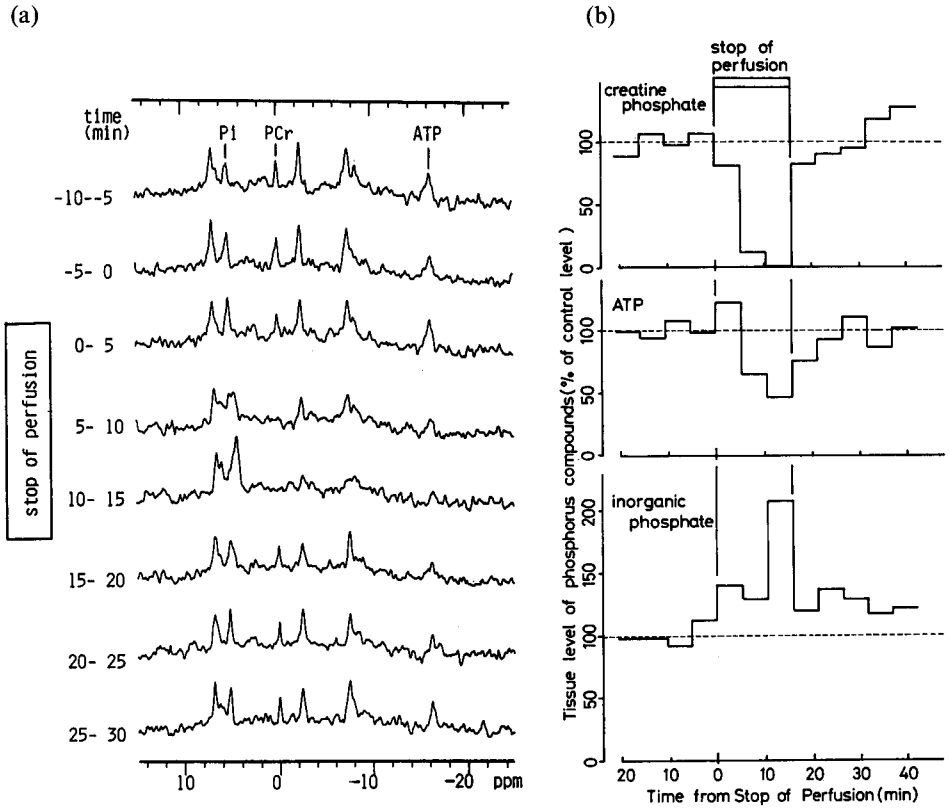

Fig. 3. Metabolic changes induced by a transient cessation of perfusion for 15 min. (a) ^{31}P NMR spectra were collected sequentially every 5 min. (b) Time course of changes in PCr, ATP, and Pi levels by cessation of perfusion, as expressed by a percentage of the resting control level of phosphorus compounds.

Effects of cessation of perfusion (Fig. 3)

The cessation of perfusion caused hypoxia of the tissue and reduced the "supply" of ATP from the oxidative metabolism. When the perfusion was stopped for 15 min, ATP and PCr decreased to 50 and 0% of the resting levels, respectively, while Pi increased to 200% of the resting level. The level of PCr decreased more quickly than the level of ATP, indicating that PCr supplies ATP rapidly via the Lohmann reaction. The resonance peak of Pi shifted to a higher magnetic field, indicating that the tissue pH decreased. After perfusion was resumed, the phosphorus compounds quickly recovered their resting levels and the peak of Pi signal shifted to its original position, indicating the recovery of tissue pH.

Effects of acetylcholine administration

Continuous stimulation with 1.0 μM ACh caused a marked salivary secretion

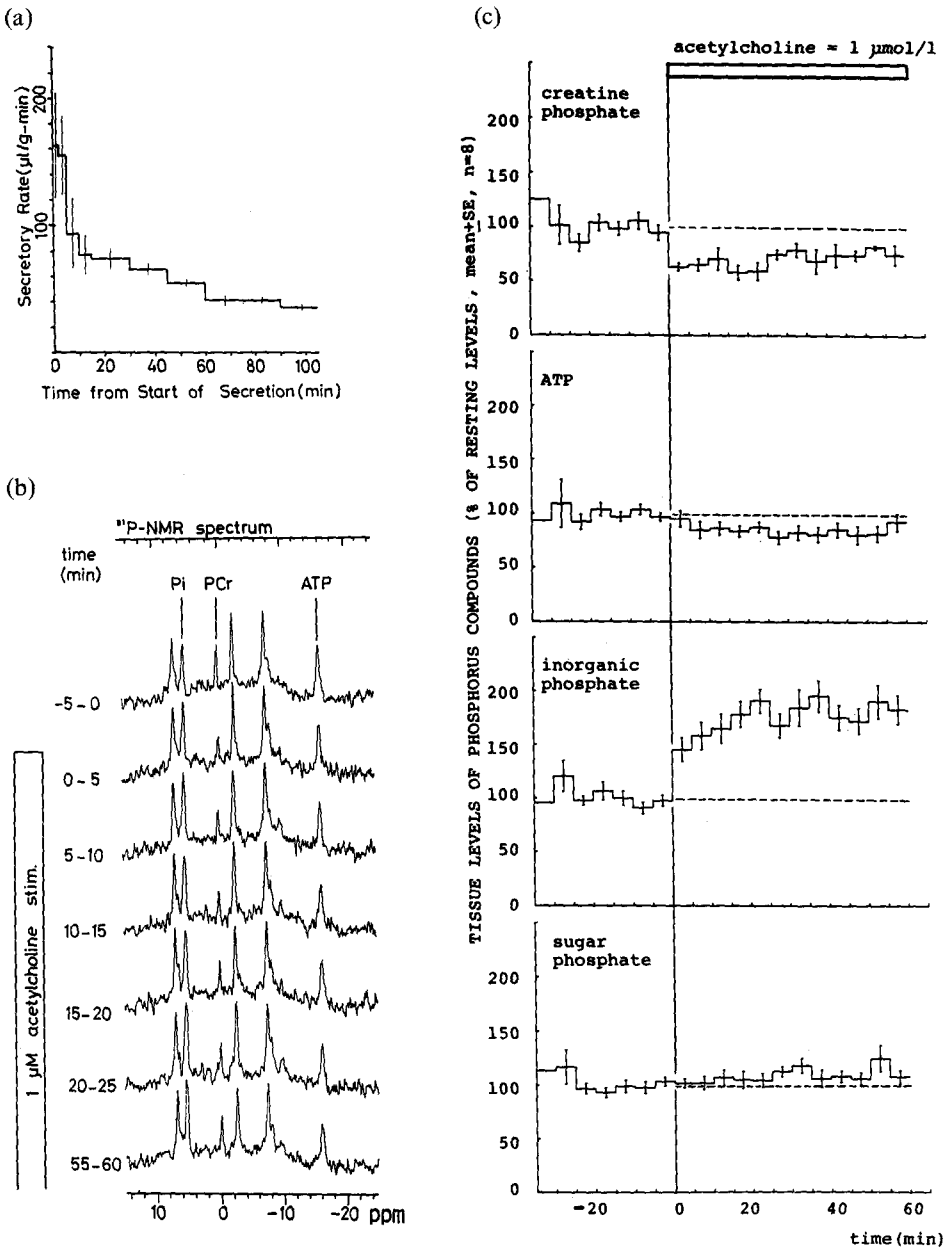

Fig. 4. Metabolic changes of the isolated perfused mandibular gland of rat (24°C) during salivary secretion induced by acetylcholine (1 μM). (a) Secretory rate of saliva (μl/(g·min), $n=4$, mean $\pm$ S.E.). (b) ^{31}P NMR spectra were taken sequentially every 5 min. (c) Time course of changes in PCr, ATP, Pi, and SP.

(Fig. 4a). The secretory flow rate reached the maximum (181 ± 24 μl/(g·min), ±S.E., $n=4$) at the initial 2 min and decreased time-dependently to the plateau level (41.6 ± 2.2 μl/(g·min), ±S.E., $n=4$, sampled at 75–90 min). The secretory rate at 24°C was about one half of that at 37°C. The optimal concentration of ACh was between 0.1 and 1 μM for the secretory flow rate.

Figure 4b shows ^{31}P NMR spectra during the secretion. The changes in the phosphorus compounds are shown as a percentage of the resting level in Fig. 4c. By the administration of ACh, the tissue level of PCr decreased quickly to $63.1 \pm 3.6\%$ (±S.E., $n=8$) of the resting level, and during secretion, the PCr gradually regained its level to $75.2 \pm 9.2\%$ (±S.E., $n=8$) of the resting value. The ATP level decreased slowly to $84.3 \pm 7.6\%$ at 5–10 min after the start of stimulation and maintained the level (80–90% of the resting level).

The level of Pi increased quickly during the initial 5 min and measured $145.2 \pm 11.3\%$ of the resting level. During the stimulation, Pi maintained the level (about 180% of the resting level). The level of SP was slightly increased by several percent of the resting level ($p<0.001$) and maintained its level during the ACh stimulation.

DISCUSSION

In most of the epithelial transport systems, Na^+/K^+ ATPase is believed to establish the Na^+ gradient across the cell membrane to create the driving force for Na^+-coupled transport systems. Recently, ^{31}P NMR has been applied to kinetic measurement of phosphorus energy metabolites in various epithelia (BALABAN *et al.*, 1981; BOND *et al.*, 1981; LIN *et al.*, 1982; NUNNALLY *et al.*, 1983). The mandibular salivary gland has several advantages for NMR measurement as follow: 1) almost all NMR signals from the gland come from acinar cells, because there is no smooth muscle but only a trace volume of myoepithelial component; 2) a simple evaluation of secretion can be achieved by measuring the amount of secreted saliva; and 3) no secretion without added secretagogues.

We have applied the ^{31}P NMR method to the isolated perfused submandibular gland of the dog (MURAKAMI *et al*, 1983, 1984; NAKAHARI *et al.*, 1985) and reported that during salivary secretion by ACh, the levels of ATP, PCr, and tissue pH decreased, the ADP level increased, and the Na-replacement suppressed these responses by ACh. However, as described above, there were several disadvantages in using the dog mandibular gland. On the other hand, many physiological, biochemical, and morphological studies on the salivary glands have been conducted using the rat (YOUNG and VAN LENNEP, 1978), and the vascular architecture is rather simple and the individual variation of laboratory rats is minimum. In addition, the isolated perfused mandibular glands of rat and rabbit can secrete as well as an *in vivo* gland (CASE *et al.*, 1980; COMPTON *et al.*, 1981; CASE and HUNTER, 1982; MARTINEZ and CASSITY, 1983).

In the present study, we applied the ^{31}P NMR method to the rat mandibular

gland, focusing especially on the determination of ATP and the effect of sustained stimulation. Comparing ^{31}P NMR spectrum of the rat gland with that of the dog gland, NTP, NDP, and PCr were similarly observed, but some differences were observed as follows. The resonances of phosphodiesters were not observed in the rat gland. The sugar phosphate of the dog gland was observed as a composite resonance of several components, but that of the rat gland was a single component. Interpretation of these differences requires further investigation.

^{31}P NMR spectroscopy can measure the amount of nucleotide phosphate but cannot discriminate the kinds of nucleotide-5′-phosphates. By HPLC, adenine and guanine nucleotides were separated for the first time in the rat mandibular gland. As a result, 80–90% of NTP's resonance reflects ATP in the mandibular gland. Thus, the tissue content of ATP was determined by HPLC as 1.64 mmol/kg wet weight. This value agreed well with the reported value, 1.24 mmol/kg wet weight in immediately frozen rat mandibular glands (DREISEBACH and GERLACH, 1967). As mentioned in RESULTS, a slight difference of ATP content was measured by HPLC, indicating that HPLC is a powerful method for precise determination of ATP content.

The ATP system is well known as the major energy carrier system and GTP is also recognized as the energy donor to several kinds of biosynthesis materials such as cellulose, porphyrin, protein, etc. (LEHNINGER, 1975). The present study suggested that about 80–90% of the total energy phosphate could be carried by ATP system and the rest by GTP system in the mandibular gland. On the other hand, UTP is known to act as a phosphate donor leading to polysaccharide synthesis, and that it possibly participates in the biosynthesis of mucin in the mandibular gland. However, uridine-5′-phosphates were not detected in the present study, suggesting that UTP level is possibly very low in the rat mandibular gland, less than the noise level of HPLC result, 0.05 mmol/kg.

The resting level of PCr in the salivary gland was reported as 0.62–1.1 mmol/kg tissue weight in the dog submandibular gland (NORTHUP, 1935; MURAKAMI *et al.*, 1983), and 0.46 mmol/kg tissue weight in the rat mandibular gland (FURUYAMA *et al.*, 1980). We estimated the tissue level of PCr as 3.3 mmol/kg from the relative PCr concentration by ^{31}P NMR and the ATP concentration by chemical analysis. The breakdown of PCr was so rapid that the chemical analysis did not allow estimation of the actual level of PCr in the *in situ* gland. In the present study, the combination of ^{31}P NMR and the chemical analysis of ATP gave the highest value of PCr among the reported values, indicating the usefulness of this procedure. The total creatine (creatine + PCr) was reported as 2.56 mmol/kg wet tissue (FURUYAMA *et al.*, 1980). The present findings suggest that most of the creatine could be in the form of creatine phosphate in the mandibular gland of the rat. FURUYAMA *et al.* (1980) also reported that the PCr level in the rat mandibular gland was as high as that in the brain, and that the creatine kinase activities occurred in the cytosolic and mitochondrial fractions. The mitochondrial creatine kinase in the rat mandibular gland was suggested to be directed to PCr formation and to be coupled with

oxidative phosphorylation (SUGIYA and SAKAI, 1982).

We used Pi in the perfusate and the venous effluent was drained freely out of the gland. Since the NMR method cannot discriminate intracellular or extracellular signals, the Pi signal in the present study was not only from the intracellular Pi but from the extracellular Pi, Pi in the perfusate and the effluent. That is, the resting value of signal intensity of Pi reflected a sum of glandular Pi and extraglandular Pi. On the other hand, the increase in Pi by ACh stimulation or by the cessation of perfusion indicated an increase in the breakdown of phosphorus energy compounds, i.e. increase in ATP hydrolysis, qualitatively. However, it is unknown whether extracellular Pi increased or not.

The existence of Na^+/K^+ ATPase was reported in the rat mandibular gland (SCHWARTZ and MOORE, 1968; BOGART, 1975), and there are many reports on the inhibitory effects by ouabain on salivary secretion (PETERSEN and POULSEN, 1967; MARTINEZ, 1971; MARTINEZ and CASSITY, 1983) and on Na^+ dependency of salivary secretion (PETERSEN, 1970; CASE and HUNTER, 1982). BURGEN (1956) and IMAI (1965) reported that ACh increased the Na^+ entry in the salivary gland. The importance of Na in the coupling between secretion and energy supply was stressed by the findings that ACh caused no change in the ATP and PCr levels during the Na-depleted perfusion (MURAKAMI *et al.*, 1984).

The short-period stimulation (1 μM of ACh for 3 min) caused no change in the ATP level of the dog mandibular gland (MURAKAMI *et al.*, 1984). Also in the present study, ATP was maintained at $94.9 \pm 7.7\%$ ($\pm$S.E., $n=8$) of the resting level at the initial 0–5 min of the secretion. Thereafter, ATP level decreased slightly during sustained stimulation. These findings suggest two possibilities: 1) the sustained secretion requires more energy than the initial secretion, and 2) ATP supply could decrease during sustained secretion. As shown in Fig. 4a, the secretory rate is maximal at the initial stage of secretion and decreases time-dependently. If the first possibility is the case, the sustained secretion could require more energy than the initial secretion. In the present experiment, ATP level was lower but maintained at the same level during sustained secretion, indicating that the ATP supply and the ATP consumption are balanced. But the rate of ATP supply is unknown. Recently we measured the oxygen consumption of the rat mandibular gland, which increased by ACh stimulation and was maintained at the same level during sustained secretion (Murakami, unpublished data), suggesting that ATP could be supplied constantly.

We wish to thank Mr. H. Hattori (National Institute for Basic Biology), and Messrs. O. Ichikawa, A. Ikeda and K. Suzuki (National Institute for Physiological Sciences) for their technical assistance. This work was partly supported by a Grant-in-Aid for Scientific Research from the Ministry of Education, Science and Culture of Japan.

REFERENCES

BALABAN, R. S., GADIAN, D. G., and RADDA, G. K. (1981) Phosphorus nuclear magnetic resonance study of the kidney *in vivo*. *Kidney Int.*, **20**: 575–579.

BOGART, B. I. (1975) Secretory dynamics of the rat submandibular gland: An ultrastructural and cytochemical study of the isoproterenol-induced secretory cycle. *J. Ultrastruct. Res.*, **52**: 139–155.

BOND, M., SHPORER, M., PETERSEN, K., and CIVAN, M. M. (1981) ^{31}P nuclear magnetic resonance analysis of toad urinary bladder. *Mol. Physiol.*, **1**: 243–263.

BURGEN, A. S. V. (1956) The secretion of potassium in saliva. *J. Physiol. (Lond.)*, **132**: 20–39.

BURT, C. T., GLONEK, T., and BARANY, M. (1976) Analysis of phosphate metabolites, the intracellular pH, and the state of adenosine triphosphate in intact muscle by phosphorus nuclear magnetic resonance. *J. Biol. Chem.*, **251**: 2584–2591.

CASE, R. M. and HUNTER, M. (1982) The dependence of secretion from the perfused rabbit mandibular salivary gland on extracellular Na^+ concentration. *J. Physiol. (Lond.)*, **326**: 39P–40P.

CASE, R. M., CONIGRAVE, A. D., NOVAK, I., and YOUNG, J. A. (1980) Electrolyte and protein secretion by the perfused rabbit mandibular gland stimulated with acetylcholine or catecholamines. *J. Physiol. (Lond.)*, **300**: 467–487.

COMPTON, J., MARTINEZ, J. R., MARTINEZ, A. M., and YOUNG, J. A. (1981) Fluid and electrolyte secretion from the isolated, perfused submandibular and sublingual glands of the rat. *Arch. Oral Biol.*, **26**: 555–561.

DREISEBACH, R. H. and GERLACH, E. (1967) Adenosine phosphate of rat salivary and lacrimal glands *in vitro*. *Proc. Soc. Exp. Biol. Med.*, **126**: 281–282.

FURUYAMA, S., ABE, M., YOKOYAMA, N., SUGIYA, H., and FUJITA, Y. (1980) Mitochondrial creatine kinase in rat submandibular gland. *Int. J. Biochem.*, **11**: 259–264.

HOLLIS, D. P., NUNNALLY, R. L., TAYLOR, G. G., WEISFELDT, M. L., IV, and JACOBUS, W. E. (1978) Phosphorus nuclear magnetic resonance studies of heart physiology. *J. Magn. Reson.*, **29**: 319–330.

HOULT, D. I., BUSBY, R. J. W., GADIAN, D. G., RADDA, G. K., RICHARDS, R. E., and SEELEY, B. J. (1974) Observation of tissue metabolites using ^{31}P nuclear magnetic resonance. *Nature*, **252**: 285–287.

IMAI, Y. (1965) Study of the secretion mechanism of the submaxillary gland of dog. Part 2. Effects of exchanging ions in the perfusate on salivary secretion and secretory potential, with special reference to the ionic distribution in the gland tissue. *J. Physiol. Soc. Jpn.*, **27**: 313–324.

LEHNINGER, A. L. (1975) Biochemistry, 2nd ed. Worth Publishers, Inc., New York, 1104 pp.

LIN, L.-E., SHPORER, M., and CIVAN, M. M. (1982) ^{31}P nuclear magnetic resonance analysis of frog skin. *Am. J. Physiol.*, **243** (*Cell Physiol.*, **12**): C74–C80.

MARTINEZ, J. R. (1971) Action of ouabain on submaxillary secretion in the dog. *J. Pharmacol. Exp. Ther.*, **178**: 616–624.

MARTINEZ, J. R. and CASSITY, N. (1983) Effect of transport inhibitors on secretion by perfused rat submandibular gland. *Am. J. Physiol.*, **245**: G711–G716.

MCLAUGHLIN, A. C., TAKEDA, H., and CHANCE, B. (1979) Rapid ATP assays in perfused mouse liver by ^{31}P NMR. *Proc. Natl. Acad. Sci. U.S.A.*, **76**: 5445–5449.

MURAKAMI, M. (1979) Measurement of heat production in dog submandibular gland. *Jpn. J. Physiol.*, **29**: 491–507.

MURAKAMI, M., IMAI, Y., SEO, Y., MORIMOTO, T., SHIGA, K., and WATARI, H. (1983) Phosphorus nuclear magnetic resonance of perfused salivary gland. *Biochim. Biphys. Acta*, **762**: 19–24.

MURAKAMI, M., SEO, Y., NAKAHARI, T., MORI, H., IMAI, Y., and WATARI, H. (1984) Effects of Na^+ depletion on fluid secretion and levels of phosphorus compounds as measured by ^{31}P-NMR in perfused canine mandibular gland. *Jpn. J. Physiol.*, **34**: 587–597.

NAKAHARI, T., SEO, Y., MURAKAMI, M., MORI, H., MIYAMOTO, S., IMAI, Y., and WATARI, H. (1985) ^{31}P-NMR study of dog submandibular gland *in vivo* and *in vitro* using the topical magnetic resoance. *Jpn. J. Physiol.*, **35**: 729–740.

NAVON, G., OGAWA, S., SHULMAN, R. G., and YAMANE, T. (1977) ^{31}P nuclear magnetic resonance studies of Ehrlich ascites tumor cells. *Proc. Natl. Acad. Sci. U.S.A.*, **74**: 87–91.

NORTHUP, D. (1935) The secretory metabolism of the salivary gland. *Am. J. Physiol.*, **114**: 46–52.

NUNNALLY, R. L., STODDARD, J. S., HELMAN, S. I., and KOKKO, J. P. (1983) Response of ^{31}P-nuclear magnetic resonance spectra of frog skin to variations in P_{CO_2} and hypoxia. *Am. J. Physiol.*, **245**: F792–F800.

PETERSEN, O. H. (1970) The importance of extracellular sodium and potassium for acetylcholine-evoked salivary secretion. *Experientia*, **26**: 1103–1104.

PETERSEN, O. H. and POULSEN, J. H. (1967) Inhibition of salivary secretion and secretory potentials by g-strophantin, dinitrophenol and cyanide. *Acta Physiol. Scand.*, **71**: 194–202.

SCHWARTZ, A. and MOORE, C. A. (1968) Highly active Na^+, K^+-ATPase in rat submaxillary gland bearing on salivary secretion. *Am. J. Physiol.*, **214**: 1163–1167.

STEWART, D. J., PON, D. J., and SEN, A. K. (1983) Cholinergic stimulation of ouabain-sensitive respiration in rat submandibular gland. *Am. J. Physiol.*, **245**: G364–G368.

SUGIYA, H. and SAKAI, T. (1982) Regulation of creatine phosphate concentration in rat submandibular gland. *Nihon Univ. J. Oral Sci.*, **8**: 138–147.

TERROUX, K. G. and BURGEN, A. S. V. (1959) Oxygen consumption and blood flow in the submaxillary gland of the dog. *Can. J. Biochem. Physiol.*, **37**: 5–15.

WATANABE, F., HASHIMOTO, T., and TAGAWA, K. (1985) Energy-independent protection of the oxidative phosphorylation capacity of mitochondria against anoxic damage by ATP and its non-metabolizable analogues. *J. Biochem.*, **97**: 1229–1234.

YOUNG, J. A. and VAN LENNEP, E. W. (1978) The Morphology of Salivary Glands, Academic Press, London, 273 pp.

The Effect of the Calcium Antagonist Nimodipine on the Gerbil Model of Experimental Cerebral Ischemia

ATSUSHI FUJISAWA, M.D., MASAYASU MATSUMOTO, M.D., TOMOHIRO MATSUYAMA, M.D., HIROKAZU UEDA, M.D., AKIO WANAKA, M.D., SHOTARO YONEDA, M.D., KAZUFUMI KIMURA, M.D., AND TAKENOBU KAMADA, M.D.

Stroke, Vol. 17, No. 4, July-August 1986

The Effect of the Calcium Antagonist Nimodipine on the Gerbil Model of Experimental Cerebral Ischemia

Atsushi Fujisawa, M.D., Masayasu Matsumoto, M.D., Tomohiro Matsuyama, M.D., Hirokazu Ueda, M.D., Akio Wanaka, M.D., Shotaro Yoneda, M.D., Kazufumi Kimura, M.D., and Takenobu Kamada, M.D.

The Effect of the Calcium Antagonist Nimodipine on the Gerbil Model of Experimental Cerebral Ischemia

ATSUSHI FUJISAWA, M.D., MASAYASU MATSUMOTO, M.D., TOMOHIRO MATSUYAMA, M.D., HIROKAZU UEDA, M.D., AKIO WANAKA, M.D., SHOTARO YONEDA, M.D., KAZUFUMI KIMURA, M.D., AND TAKENOBU KAMADA, M.D.

SUMMARY **The gerbil model was used to assess the therapeutic effects of the calcium antagonist nimodipine on cerebral ischemia. Transient cerebral ischemia was produced in each gerbil by bilateral common carotid occlusion of 10-, 15- or 20-min duration. Nimodipine (0.01 or 0.1 mg/kg) was administered intraperitoneally just before the carotid occlusion or 10–30 min after the removal of the arterial clips. Morbidity of each animal was evaluated using the stroke index, and the sum of stroke indices was calculated for evaluating the overall morbidity during a particular period of reperfusion. Mortality was observed for 24 hours after clip removal. Although, depending on the timing of the drug administration, the low-dose (0.01 mg/kg) nimodipine worsened the morbidity in the gerbils with 10-min ischemia, the high-dose (0.1 mg/kg) of the drug had a clear beneficial effect on the mortality associated with cerebral ischemia. These results are considered worthwhile for further trials to assess the usefulness of nimodipine as a therapeutic agent in the management of the acute ischemic stroke.**

Stroke Vol 17, No 4, 1986

RECENTLY there has been increasing interest in the pathophysiological role of calcium in ischemic brain injury.[1–4] Calcium has been implicated in the final common pathway not only for contraction of vascular smooth muscle in a variety of pathophysiological conditions,[5] but also for cell death caused by membrane degradation.[6, 7] It seems justified, therefore, to consider whether calcium entry blockers may have therapeutic effects on ischemic brain injury.

Amongst several calcium antagonists, nimodipine [BAY e 9736, isopropyl (2-methoxyethyl)-1,4-dihydro-2,6-dimethyl-4(3-nitrophenyl)-3,5-pyridinedi-carboxylate] has been shown to be one of the most promising ones with a preferential action on cerebral blood vessels.[8, 9] Kazda et al[10] suggested that nimodipine prevents the postischemic impairment of reperfusion following 7-min global cerebral ischemia in cats, and Hoffmeister et al[11] showed in the same model, that the circulatory effects are paralleled by improvement of functional recovery with increased survival rates. Following these studies, several investigations[12–16] were reported on the pathophysiological effects of this drug on cerebral ischemia.

The mongolian gerbil (Meriones unguiculatus), which lacks a functional connection between the carotid and vertebrobasilar arterial circulations,[17, 18] has great advantages for the screening of compounds as protective agents against brain ischemia.[19–23] There have been, however, no reports on the effects of nimodipine on the gerbil model of cerebral ischemia. In the present study, by assessing the changes both in morbidity and mortality following temporary bilateral common carotid occlusion in gerbils with nimodipine or vehicle treatment, we attempted to evaluate the therapeutic potency of the drug in the acute phase of ischemic stroke.

Methods

A total of 202 adult Mongolian gerbils of both sexes weighing 60–80 g were used in the present study. The gerbils were anesthetized with ketamine hydrochloride (Ketalar®, 50 mg/kg i.p.) and placed in the supine position. Bilateral common carotid arteries were then exposed through a ventral midline incision of the neck, and were looped with silk sutures. As the gerbils emerged from the anesthetic, the two common carotid arteries were occluded simultaneously by pulling the sutures around them and thereafter they were occluded by aneurysmal clips for 10, 15 or 20 min. Following these ischemic periods, the clips were removed to restore the blood flow and the patency of the arteries was ascertained by visual inspection. After this, the animals were returned to their cages again for recovery and observation. Morbidity and mortality were evaluated and scored by an evaluator who was blinded as to the duration of cerebral ischemia, the drug or the dosage used. Morbidity of each animal was evaluated every one hour using the McGraw's method.[19] The neurological signs included ptosis, paucity of movements, cocked head, circling behavior, splayed hindlimb, seizure and coma, and were tabulated as the stroke index such that a higher score indicated a more severe neurological deficit. We further calculated the sum of stroke indices in each gerbil for evaluating the morbidity of a particular period of reperfusion. The number of deaths in each category was ascertained 24 hours after clip removal. In order to compare the animals receiving nimodipine with the control animals receiving vehicle, life tables were also constructed by actuarial methods to indicate the cumulative probability of dying as influenced by a specific time following the ischemic insult. In all animals which survived 24-

From the Division of Angiology, First Department of Internal Medicine, Osaka University Medical School, Osaka 553, Japan.

Address correspondence to: Masayasu Matsumoto, M.D., Division of Angiology, First Department of Internal Medicine, Osaka University Medical School, Fukishima, 1 chome, Fukishima-ku, Osaka 553, Japan.

Received March 20, 1985; revision #2 accepted October 9, 1985.

TABLE 1 *The Sum of Stroke Indices Obtained at 1–6 Hours after 10, 15 and 20 Min of Bilateral Carotid Arterial Occlusion in Gerbils Treated with Vehicle or Nimodipine*

Treatment	Duration of Bilateral Carotid Occlusion		
	10 min	15 min	20 min
Vehicle	19.3 ± 3.2	50.4 ± 7.6	66.1 ± 7.1
Nimodipine (0.01 mg/kg)			
before carotid occlusion	56.6 ± 4.0*	65.1 ± 5.2	81.2 ± 5.1
10 min after reperfusion	45.5 ± 3.7*	62.0 ± 4.6	83.7 ± 13.9
30 min after reperfusion	36.0 ± 5.1*‡	60.0 ± 3.5	59.8 ± 4.5†
Nimodipine (0.1 mg/kg)			
before carotid occlusion	14.8 ± 5.1	53.3 ± 7.6	67.1 ± 6.6
10 min after reperfusion	29.3 ± 6.2	57.3 ± 4.2	73.2 ± 4.4
20 min after reperfusion	—	—	62.9 ± 9.2
30 min after reperfusion	46.0 ± 5.2*‡	57.3 ± 5.0	60.2 ± 8.4

Each value represents mean ± S.E.M. For the number of animals in each group, see table 2 or 3.
*$p < 0.01$; significantly different from the gerbils with vehicle treatment. †$p < 0.05$, ‡$p < 0.01$; significantly different from the gerbils with nimodipine treatment before bilateral carotid occlusion. Statistical significance was determined by the unpaired t-test.

hour reperfusion after global cerebral ischemia, the existence of forebrain ischemia during bilateral common carotid occlusion was confirmed by the carbon black perfusion method.[18]

The treatment consisted of a single intraperitoneal injection of either nimodipine (0.01 or 0.1 mg/kg) or vehicle just prior to bilateral carotid occlusion or 10–30 min after reestablishment of cerebral blood circulation. The volume of injection was the same (0.1 ml) for each gerbil. The vehicle contained, per liter of solution, 200 g 96% ethanol, 170 g polyethyleneglycol 400, 2g sodium citrate, and 0.5 g citric acid. Because nimodipine is very sensitive to white light, the drug was always dispensed under sodium light and the syringe for injection was always covered in aluminum foil. Each drug and dose was also administered to 5 gerbils without carotid occlusion to verify the absence of toxicity in the dosage selected.

Results

There were no intraoperative deaths among the gerbils. The morbidity for each treatment group was represented by the sum of stroke indices obtained at 1–6 hours after bilateral common carotid occlusion, and summarized in table 1. In the gerbils with 15- or 20-min bilateral cerebral ischemia, there was no significant difference in the sum of stroke indices between the nimodipine-treated and vehicle-treated animals though the tendency of decrease of stroke indices was noted in the gerbils with nimodipine treatment that survived 24-hour reperfusion. On the other hand, in the gerbils with 10-min ischemia, significant increase of the morbidity scores was observed in the groups treated with the low-dose (0.01 mg/kg) nimodipine and the group with the high-dose (0.1 mg/kg) nimodipine 30 min after reperfusion. Depending on the timing of the administration of the drugs, significant differences were observed in the morbidity even among the gerbils with the same dose of nimodipine.

Mortality rates for each treatment group are summarized in table 2. Although a significant increase of mortality rate was observed in 10-min ischemic gerbils with the low-dose nimodipine just before bilateral common carotid occlusion, no significant differences were noted in mortality rate between the vehicle-treated gerbils and the remaining nimodipine-treated animals with 10-min ischemia, and no significant effects of nimodipine on mortality rate were observed in 15-min ischemic gerbils. On the other hand, significant decrease of mortality rate was observed in the 20-min ischemic gerbils with the high-dose nimodipine, as compared to the vehicle-treated controls. This beneficial effect of the high-dose nimodipine on the mortality rate of the 20-min ischemic gerbils was clearly demonstrated in figure 1. With respect to the 20-min ischemic gerbils, there were no significant differences in the probability of dying among the low-dose nimodipine-treated groups and among the high-dose nimodipine-

TABLE 2 *Mortality Rates at 24 Hours after 10, 15 and 20 Min of Bilateral Carotid Arterial Occlusion in Gerbils Treated with Vehicle or Nimodipine*

Treatment	Duration of Bilateral Carotid Occlusion		
	10 min	15 min	20 min
Vehicle	13% (15)	58% (12)	100% (11)
Nimodipine (0.01 mg/kg)			
before carotid occlusion	73%* (11)	80% (10)	100% (10)
10 min after reperfusion	50% (4)	80% (5)	100% (3)
30 min after reperfusion	17% (12)	63% (8)	100% (4)
Nimodipine (0.1 mg/kg)			
before carotid occlusion	10% (10)	40% (10)	60%* (10)
10 min after reperfusion	0% (10)	50% (10)	80% (10)
20 min after reperfusion	—	—	60%* (10)
30 min after reperfusion	0% (6)	50% (6)	60%* (10)

Each value represents percent mortality at 24 hours after bilateral cerebral ischemia. The number of animals in each group is given in parentheses. *$p < 0.05$; significantly different from the gerbils with vehicle treatment. Statistical significance was determined by the chi-square test.

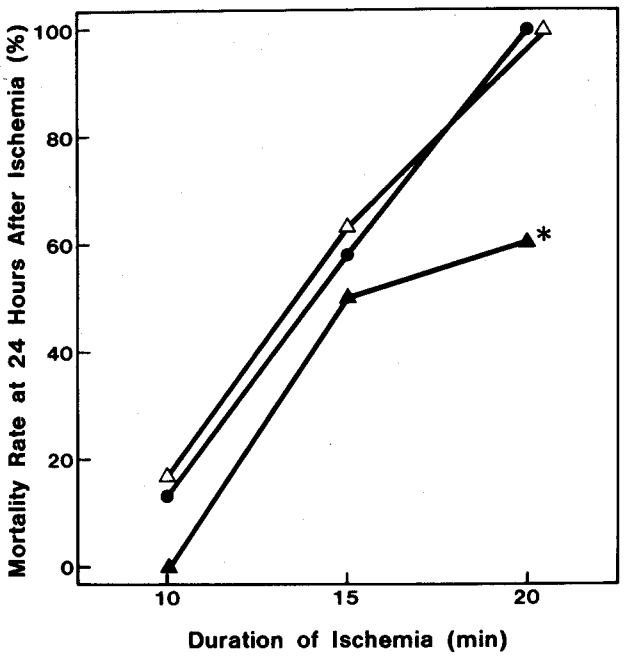

FIGURE 1. *Comparison of mortality curves among the vehicle-treated gerbils (●) and the gerbils with 0.01 mg/kg (△) and 0.1 mg/kg (▲) nimodipine treatment at 30 min after clip removal. Significant difference ($\chi^2 = 5.46$, $p < 0.05$) from the vehicle-treated control animals was indicated by the asterisk (★). Statistical significance was determined by the chi-square test. No significant difference was observed in mortality rate between the vehicle-treated and 0.01 mg/kg nimodipine-treated animals.*

treated ones. Therefore, these groups were combined and analyzed as a single group. Figure 2 presents the life tables for the three treatment groups with 20-min bilateral cerebral ischemia. No significant improvement was observed in the gerbils with the low-dose nimodipine but the gerbils treated with the high-dose nimodipine proved to have a significantly lower probability of dying than the vehicle-treated gerbils at 7–24 hours after reperfusion.

The gerbils with cerebral ischemia often showed seizures, which in turn could affect survival. We therefore checked the incidence of seizures in each group of gerbils and summarized the results in table 3. The gerbils with longer duration ischemia showed higher incidence of seizures. There were no significant differences in incidence of seizures between the vehicle-treated and nimodipine-treated gerbils, except for 10-min ischemic gerbils with the low-dose nimodipine treatment that showed an increased incidence of seizures during the early recovery period.

Discussion

In recent years, the model of transient bilateral cerebral ischemia in the gerbil has been intensively used for testing therapeutic agents in the management of the acute brain ischemia.[20–23] Bilateral common carotid occlusion produces a fairly uniform ischemia in the telencephalon without ambiguity[18, 24, 25] and the surgical procedure is so simple that large number of animals can be assessed statistically. The transient ischemic model can also allow vascular access of administered drugs or improved blood flow to affect the ischemic areas of the brain. In the previous experiments,[26] we characterized the morbidity and established a mortality curve during the duration of ischemia as the dependent variable in this model of transient global cerebral ischemia. Bilateral common carotid artery occlusion resulted in 100% mortality during a 24-hour period in the gerbils subjected to 20-min occlusion, whereas negligible mortality was associated with the bilateral carotid occlusion of 10-min duration. In the present study, we introduced a single administration of nimodipine (0.01 or 0.1 mg/kg) or vehicle as independent variables to determine possible changes in the morbidity and the mortality curve following the identical periods of bilateral common carotid occlusion.

There is no doubt that the outcome of cerebral ischemia can be influenced by the calcium antagonist nimodipine as indicated by the present results. This study also indicates that the effectiveness depended not only on the dose of nimodipine but also on the timing of the drug administration. As a matter of fact, the detrimental effects of the low-dose nimodipine were unexpectedly observed in the gerbils with 10-min

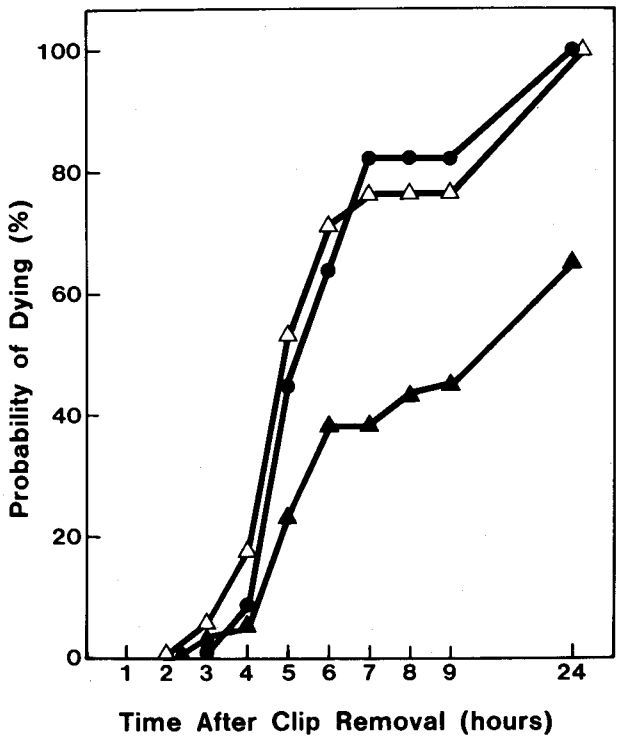

FIGURE 2. *Actuarial tables for the three treatment groups (i.e., 11 gerbils with vehicle (●), 17 with 0.01 mg/kg nimodipine (△) and 40 with 0.1 mg/kg nimodipine (▲)) after 20-min bilateral cerebral ischemia. Significant differences by the chi-square test were observed in probability of dying between the vehicle-treated and 0.1 mg/kg nimodipine-treated gerbils at 7 ($\chi^2 = 6.72$, $p < 0.01$), 8 ($\chi^2 = 4.75$, $p < 0.05$), 9 ($\chi^2 = 4.28$, $p < 0.05$) or 24 hours ($\chi^2 = 5.25$, $p < 0.05$) after ischemic episode.*

TABLE 3 *Incidence of Seizures during 6-hour Reperfusion after 10, 15 and 20 Min of Bilateral Carotid Arterial Occlusion in Gerbils Treated with Vehicle or Nimodipine*

Treatment	Duration of Bilateral Carotid Occlusion		
	10 min	15 min	20 min
Vehicle	13% (15)	75% (12)	82% (11)
Nimodipine (0.01 mg/kg)			
before carotid occlusion	64%* (11)	70% (10)	100% (10)
10 min after reperfusion	50% (4)	80% (5)	100% (3)
30 min after reperfusion	42% (12)	75% (8)	75% (4)
Nimodipine (0.1 mg/kg)			
before carotid occlusion	20% (10)	70% (10)	90% (10)
10 min after reperfusion	20% (10)	90% (10)	100% (10)
20 min after reperfusion	—	—	80% (10)
30 min after reperfusion	17% (6)	33% (6)	70% (10)

Each value represents percent incidence of seizures during 6-hour reperfusion after bilateral cerebral ischemia. The number of animals in each group is given in parentheses. *$p < 0.01$; significantly different from the gerbils with vehicle treatment ($\chi^2 = 7.13$). Statistical significance was determined by the chi-square test.

ischemia, especially when the drug was injected just before the carotid occlusion (tables 1, 2 and 3). On the other hand, clear beneficial effects of the high-dose nimodipine were observed in the gerbils with 20-min ischemia, irrespective of the time of administration — whether given prior to or after termination of the ischemic episode (table 2, figs. 1 and 2).

Although it is very difficult to explain the exact mechanism of these effects of nimodipine, the effects of this drug on the postischemic reperfusion of the ischemic brain[10, 11, 15, 16] seemed to be one of the major factors which determine the outcome of the ischemic gerbils. In our preliminary experiment, a single intraperitoneal injection of 0.01 or 0.1 mg/kg nimodipine reduced mean arterial pressure, which was continuously monitored with an intra-aortic catheter, by 3–7% for about 15 min or by 7–20% for more than 30 min, respectively. In this model of cerebral ischemia, significant regional or systemic hemodynamic changes were reported both during and after bilateral cerebral ischemia.[21, 24, 27, 28] An initial fall of mean blood pressure, which may cause secondary impairment of cerebral blood flow, was observed soon after the release of the aneurysmal clips.[21, 28] Therefore, it seems to be most probable that when administered just before the carotid occlusion in 10-min ischemic gerbils, the low-dose nimodipine produced only the potentiation of the initial fall of blood pressure after clip removal because of the shorter duration of action and the weaker effects on cerebral blood flow, and showed the detrimental effects on morbidity and mortality through the impairment of the postischemic reperfusion. Even if this dose of nimodipine still has a selective action on brain vessels[29] during the occlusion of both the carotids, there are almost no functional collateral pathways[17, 18] through which drugs can affect the vessels in the ischemic brain regions, and immediately after the recirculation strong postischemic dilatation of these vessels can be seen without vasodilatory drugs.[30, 31] A different time schedule experiment was then added to clarify this point. A significant difference, detected in morbidity and mortality between the gerbils with the low-dose nimodipine treatment before carotid occlusion and at 30 min after reperfusion, supports the above-mentioned suggestion. However it may be the ischemia-produced seizures, and not the lowered blood pressure per se, which more directly accounts for reduced survival in the lower dose regime. As shown in tables 2 and 3, a clear association between seizures and outcome was observed and the ineffective and sometimes harmful dose schedule of nimodipine was indeed accompanied by increased seizures in the early recovery period which might be caused by the fall in blood pressure. But other mechanisms such as the metabolic effects of nimodipine[32] cannot be wholly excluded and, in the primate model of focal cerebral ischemia, it was suggested that nimodipine increases the susceptibility of tissue to ischemic damage in the areas where blood flow is critically reduced.[13]

On the other hand, the high-dose nimodipine has a greater modifying effect of longer duration on regional cerebral blood flow than the low-dose;[29, 33] this may be a major factor responsible for the observed differences in the survival of the gerbils (table 2, figs. 1 and 2). Our results obtained in the gerbils with the high-dose nimodipine were in agreement with the previous reports.[11, 14–16] A consistent finding in previous experiments and in ours has been that treatment with nimodipine improves survival after ischemic cerebral damage. In order to understand how nimodipine may benefit the gerbils with predicted 100% mortality, we should know the pathophysiological cause of death. As mentioned above, the lethality of prolonged cerebral ischemia may be, in part, related to the metabolic harm from the seizures triggered by the cerebral ischemia. But the benefits of the higher dose regime cannot be explained by control of seizures, because no significant difference was detected in the incidence of seizures between the gerbils with vehicle treatment and those with high-dose nimodipine treatment (table 3). Avery et al[34] recently reported that in this model of transient global cerebral ischemia, mortality correlated well with the evolution of cerebral edema. In our investigation,[26] we also could detect significant differences in specific gravity between the ischemic telencephalic brain regions from the dying animals and the others. This lethal edema process could resolve with reperfusion when the postischemic impairment of cerebral blood flow, which might be responsible for a large part of the ultimate brain damage,[1, 15, 16] was ameliorated in the gerbils with nimodipine treatment. The present results also indicate that nimodipine need not be given pre-ischemia to improve the outcome of severe transient cerebral ischemia.

We conclude that nimodipine has beneficial effects in the gerbil model of cerebral ischemia when administered in an adequate dosage and with proper timing. This drug should be considered seriously for further therapeutic trials of acute ischemic stroke.

Acknowledgments

We wish to express our thanks to Mr. Y. Suzuki (Research Institute, Ono Pharmaceutical, Osaka) for thorough management of animals, and Miss F. Itoh and M. Habuchi for their secretarial assistance. Nimodipine and vehicle were generously supplied by Bayer Yakuhin, Ltd., Osaka, Japan.

References

1. Siesjö BK: Cell damage in the brain: A speculative synthesis. J Cereb Blood Flow Metab **1:** 155–185, 1981
2. Hass W: Beyond cerebral blood flow, metabolism and ischemic thresholds: An examination of the role of calcium in the initiation of cerebral infarction. *In:* Meyer JS, Lechner H, Reivich M, Otto EO, Aranibar A, eds. Proc 10th Salzburg Conference, Cerebral Vascular Disease 3. Amsterdam/Oxford/Princeton: Excerpta Medica, 3–17, 1981
3. Yanagihara T, McCall JT: Ionic shift in cerebral ischemia. Life Sci **30:** 1921–1925, 1982
4. Simon RP, Griffiths T, Evans MC, Swan JH, Meldrum BS: Calcium overload in selectively vulnerable neurons of the hippocampus during and after ischemia: An electron microscopy study in the rat. J Cereb Blood Flow Metab **4:** 350–361, 1984
5. Bolton TB: Mechanisms of action of transmitters and other substances on smooth muscle. Physiol Rev **59:** 606–718, 1979
6. Schanne FAX, Kane AB, Young EE, Farber JL: Calcium dependence of toxic cell death: A final common pathway. Science **206:** 700–702, 1979
7. Siesjö BK: Cerebral circulation and metabolism. J Neurosurg **60:** 883–908, 1984
8. Kazda S, Towart R: Nimodipine: a new calcium antagonistic drug with a preferential cerebrovascular action. Acta Neurochir **63:** 259–265, 1982
9. Towart R: The selective inhibition of serotonin-induced contractions of rabbit cerebral vascular smooth muscle by calcium-antagonistic dihydropyridines. Circ Res **48:** 650–657, 1981
10. Kazda S, Hoffmeister F, Garthoff B, Towart R: Prevention of the post-ischaemic impaired reperfusion of the brain by nimodipine (BAY e 9736). Acta Neurol Scand **60** [Suppl 72]: 302–303, 1979
11. Hoffmeister F, Kazda S, Krause HP: Influence of nimodipine (BAY e 9736) on the postischaemic changes of brain function. Acta Neurol Scand **60** [Suppl 72]: 358–359, 1979
12. Harper AM, Craigen L, Kazda S: Effect of the calcium antagonist, nimodipine, on cerebral blood flow and metabolism in the primate. J Cereb Blood Flow Metab **1:** 349–356, 1981
13. Harris RJ, Branston NM, Symon L, Bayhan M, Watson A: The effects of a calcium antagonist, nimodipine, upon physiological responses of the cerebral vasculature and its possible influence upon focal cerebral ischemia. Stroke **13:** 759–766, 1982
14. Kazda S, Garthoff B, Luckhaus G, Nash G: Prevention of cerebrovascular lesions and mortality in stroke-prone spontaneously hypertensive rats by the calcium antagonist nimodipine. *In:* Goldfraind T, Albertini A, Paoletti R, eds. Calcium Modulators. Amsterdam: Elsevier Biomedical Press, 155–167, 1982
15. Steen PA, Newberg LA, Milde JH, Michenfelder JD: Nimodipine improves cerebral blood flow and neurologic recovery after complete cerebral ischemia in the dog. J Cereb Blood Flow Metab **3:** 38–43, 1983
16. Steen PA, Newberg LA, Milde JH, Michenfelder JD: Cerebral blood flow and neurologic outcome when nimodipine is given after complete cerebral ischemia in the dog. J Cereb Blood Flow Metab **4:** 82–87, 1984
17. Donadio MF, Kozlowski PB, Kaplan H, Wisniewski HM, Majkowski J: Brain vasculature and induced ischemia in seizure-prone and non-seizure-prone gerbils. Brain Res **234:** 263–273, 1982
18. Matsuyama T, Matsumoto M, Fujisawa A et al: Why are infant gerbils more resistant than adults to cerebral infarction after carotid ligation? J Cereb Blood Flow Metab **3:** 381–385, 1983
19. McGraw CP: Experimental cerebral infarction. Effects of pentobarbital in Mongolian gerbils. Arch Neurol **34:** 334–336, 1977
20. Jarrott DM, Domer FR: A gerbil model of cerebral ischemia suitable for drug evaluation. Stroke **11:** 203–209, 1980
21. Holaday JW, D'Amato RJ: Naloxone or TRH fails to improve neurologic deficits in gerbil models of "stroke." Life Sci **31:** 385–392, 1982
22. Taylor MD, Palmer GC, Callahan III AS: Protective action by methylprednisolone, allopurinol and indomethacin against stroke-induced damage to adenylate cyclase in gerbil cerebral cortex. Stroke **15:** 329–335, 1984
23. Black KL, Hsu S, Radin NS, Hoff JT: Sodium 5-(3′-pyridinylmethyl) benzofuran-2-carboxylate (U-63557A) potentiates protective effect of intravenous eicosapentaenoic acid on impaired CBF in ischemic gerbils. J Neurosurg **61:** 453–457, 1984
24. Matsumoto M, Matsuyama T, Fujisawa A, Yoneda S, Kimura K, Abe H: Hemodynamic studies in the gerbil stroke model: Age-related changes in incidence of cerebral ischemia and changes in systemic or regional hemodynamics after bilateral common carotid artery occlusion. J Cereb Blood Flow Metab **3** [Suppl 1]: S337–S338, 1983
25. Matsumoto M, Kimura K, Fujisawa A et al: Differential effect of cerebral ischemia on monoamine content of discrete brain regions of the Mongolian gerbil (Meriones unguiculatus). J Neurochem **42:** 647–651, 1984
26. Fujisawa A, Matsumoto M, Matsuyama T, Yoneda S, Kimura K: Changes in specific gravity of discrete brain regions and postischemic morbidity following reversible and irreversible cerebral ischemia in Mongolian gerbil. *In:* Proceedings of the 6th International Symposium on Brain Edema. Berlin/Heidelberg/New York: Springer-Verlag, 1985 (in press)
27. Matsumoto M, Kimura K, Fujisawa A et al: Cerebral ischemic response-like hemodynamic changes induced by telencephalic ischemia in Mongolian gerbils (Meriones unguiculatus). Brain Res **294:** 367–369, 1984
28. Harrison MJG, Sedal L, Arnold J, Ross Russell RW: No-reflow phenomenon in the cerebral circulation of the gerbil. J Neurol Neurosurg Psychiatry **38:** 1190–1193, 1975
29. Kazda S, Garthoff B, Krause HP, Schlossmann K: Cerebrovascular effects of the calcium antagonistic dihydropyridine derivative nimodipine in animal experiments. Arzneimittelforsch **32:** 331–338, 1982
30. Osburne RC, Halsey JH: Cerebral blood flow — A predictor of recovery from ischemia in the gerbil. Arch Neurol **32:** 457–461, 1974
31. Iannotti F, Hoff J: Ischemic brain edema with and without reperfusion: An experimental study in gerbils. Stroke **14:** 562–567, 1983
32. d'Avella D, Cicciarello R, La Torre F et al: The effect of the calcium antagonist nimodipine upon local cerebral glucose utilization in the rat brain. Life Sci **34:** 2583–2588, 1984
33. Rosenblum WI: Effects of calcium channel blockers on pial vascular responses to receptor mediated constrictors. Stroke **15:** 284–287, 1984
34. Avery S, Crockard HA, Ross Russell R: Evolution and resolution of edema following severe temporary cerebral ischemia in the gerbil. J Neurol Neurosurg Psychiatry **47:** 604–610, 1984